

Article

Ecosystem Recovery in Progress? Initial Nutrient and Phytoplankton Response to Nitrogen Reduction from Sewage Treatment Upgrade in the San Francisco Bay Delta

Patricia M. Glibert^{1,*}, Frances P. Wilkerson², Richard C. Dugdale² and Alexander E. Parker³

¹ Horn Point Laboratory, University of Maryland Center for Environmental Science, P.O. Box 775, Cambridge, MD 21613, USA

² Estuary and Ocean Science Center, Romberg Tiburon Campus, San Francisco State University, 3150 Paradise Drive, Tiburon, CA 94920, USA

³ Department of Sciences and Mathematics, California State University Maritime Academy, 200 Maritime Academy Drive, Vallejo, CA 94590, USA

* Correspondence: glibert@umces.edu; Tel.: +1-410-221-8422

Abstract: The San Francisco Bay Delta has been an estuary of low productivity, with causes hypothesized to relate to light limitation, grazing by invasive clams, and polluting levels of NH_4^+ discharge from a wastewater treatment plant. Suppression of phytoplankton NO_3^- uptake by NH_4^+ has been well documented, and thus this estuary may have experienced the counterintuitive effect of depressed productivity due to wastewater NH_4^+ enrichment. In 2021, a new wastewater treatment plant came online, with a ~75% reduction in nitrogen load, and within-plant nitrification, converting the discharge to NO_3^- . The expectation was that this change in nitrogen loading would support healthier phytoplankton production, particularly of diatoms. Here, responses of the post-upgrade Bay Delta phytoplankton were compared to five years of data collected pre-upgrade during the fall season. Indeed, increased chlorophyll *a* accumulation in the estuary was documented after the implementation of the upgraded wastewater treatment and photophysiological responses indicated comparatively less stress. Major differences in river flow were also observed due to drought conditions during the decade covered by this study. While short-term favorable effects were observed, understanding longer-term ecological feedback interactions that may follow from this major nutrient change under variable flow conditions will require more years of observations.

Keywords: Bay Delta; ammonium; wastewater; nutrients; diatoms; F_v/F_m ; photophysiology; estuary recovery



Citation: Glibert, P.M.; Wilkerson, F.P.; Dugdale, R.C.; Parker, A.E. Ecosystem Recovery in Progress? Initial Nutrient and Phytoplankton Response to Nitrogen Reduction from Sewage Treatment Upgrade in the San Francisco Bay Delta. *Nitrogen* **2022**, *3*, 569–591. <https://doi.org/10.3390/nitrogen3040037>

Academic Editor: Rosa María Martínez-Espinosa

Received: 25 August 2022

Accepted: 8 October 2022

Published: 13 October 2022

Publisher's Note: MDPI stays neutral with regard to jurisdictional claims in published maps and institutional affiliations.



Copyright: © 2022 by the authors. Licensee MDPI, Basel, Switzerland. This article is an open access article distributed under the terms and conditions of the Creative Commons Attribution (CC BY) license (<https://creativecommons.org/licenses/by/4.0/>).

1. Introduction

The San Francisco Bay Delta has long been considered an estuary of High Nutrient-Low Growth (HNLG) [1–3]. The low productivity condition has not always been the case, as annual summer blooms with chlorophyll *a* ($\text{chl } a$) $> 20 \mu\text{g L}^{-1}$ occurred in the 1970s [4] especially during drought periods [5,6]. In recent years, phytoplankton blooms have been a relative rarity, although occasional blooms have occurred, typically dominated by the centric diatom, *Aulacoseira granulata*, e.g., [7–9]. For example, an extensive bloom of *A. granulata* was observed in the northern Bay Delta in spring 2016 [10]. Due to comparative infrequency of algal blooms, the Bay Delta has been considered to be immune from conditions of eutrophication. On the one hand, this is positive, in that conditions of large blooms and prolonged hypoxia are not problematic. On the other hand, the condition of low $\text{chl } a$ has been considered to be limiting for food availability for major fish species, leading to a condition referred to as the pelagic organism decline [11,12]. The exception to the low productivity condition in the Bay Delta is the region of the central Delta and confluence of the Sacramento and San Joaquin Rivers, where blooms of the cyanobacterium

Microcystis aeruginosa have been a recurring feature for more than two decades, e.g., [13–15]. Production of cyanobacterial blooms are not supportive of fish production.

A major source of nutrients to the Bay Delta since the early 1980s has been a wastewater treatment plant (WWTP) located in the upper Sacramento River. This WWTP discharged nitrogen (N) to the Sacramento River at the rate of 14–15 tons day⁻¹ and at concentrations at the point of discharge that increased from ~10 mg L⁻¹ when the plant came online in the early 1980s to >30–40 mg L⁻¹ in the 2000s [5,16,17]. Under average flow conditions, >90% of the total N in the northern San Francisco Estuary originated from this single source [5]. Importantly, this N was discharged in the form of NH₄⁺. The Sacramento River served as a region of nitrification, inferred from both water column changes in concentrations of NH₄⁺ and NO₃⁻ [18] and the presence of nitrifying bacteria and archaea [19,20]. Agricultural sources also supply nutrients to the Bay Delta [21–23].

The NH₄⁺ originating from the WWTP has been hypothesized to be suppressive or repressive for phytoplankton growth, rather than stimulatory [1,7–9,24,25], although this has been a topic of considerable debate, e.g., [26–28]. While NH₄⁺ can be a preferred form of N for phytoplankton, at high levels it can be toxic for cell growth [29] (and references therein). The phenomenon of productivity suppression in the presence of elevated NH₄⁺ has been observed in other rivers, lakes, estuarine and coastal ecosystems impacted by either WWTP effluent or fertilizer runoff [3,30–33]. The same phenomenon of reduced growth with elevated NH₄⁺ has also been observed in higher plants and is known as the “NH₄⁺ syndrome” [34,35].

Beginning in 2015, new discharge requirements were imposed on the Sacramento River WWTP, necessitating the building of a major new treatment plant. Servicing over 1.6 million people, the new discharge permit required that NH₄⁺ be removed from discharge, and that total N discharge be reduced by 75%, with a river discharge of 181 million gallons per day (=685 million liters per day, average dry weather amount) [36]. No requirements for a change in PO₄³⁻ discharge were imposed. Thus, with reduced N loads, the dissolved inorganic N:dissolved inorganic P (DIN:DIP) was reduced accordingly. Biological nutrient removal was added and advanced filtration removed many smaller particles that were also discharged in the pre-upgrade effluent. The upgraded WWTP—a nearly USD2 billion investment—known as the EchoWater Project (<https://www.regionalsan.com/echowater-project>, accessed on 1 May 2022) was fully implemented by late spring 2021 and represents one of the largest plants in the USA.

An alternative hypothesis for persistent low productivity in the Bay Delta is that the phytoplankton are light limited [37–39]. Due to high suspended particulate matter caused by river inflow as well as turbulence due to tides and waves [40], light availability can be poor. However, suspended particulate matter varies considerably with bay region and season, being highest during the winter and spring wet period, leading to lowest light availability during these seasons [41]. Additionally, biomass accumulation may be controlled by aggressive benthic grazing predominantly by the invasive clam, *Potamocorbula amurensis* [6,42,43]; *P. amurensis* = *Corbula amurensis*, [44]. Grazing by clams is highest in late summer/fall.

Over the past decade, California has also experienced periods of major drought, with a few years during which drought conditions were alleviated. Drought has significant impacts on waters of the Bay Delta by altering residence times, which, in turn, may allow for more in situ phytoplankton growth, which, unless grazed, would be more likely to accumulate. Conversely, for periods of high flow, it has previously been suggested that phytoplankton growth may be limited due to the short transport times in the river/estuary [45,46]. During drought there is also less dilution of effluent nutrients, potentially leading to more localized impacts. The timing of final implementation of EchoWater occurred during the most recent—and ongoing—drought.

The overarching hypothesis that will be tested over the coming years is that if the high loads of NH₄⁺ were indeed suppressive to phytoplankton growth, then an increase in phytoplankton growth should be seen when these loads are reduced. Furthermore, shifting

the form of N to NO_3^- should favor the growth of diatoms, as they are considered NO_3^- opportunists [29]. An increase in diatom production would also be expected from the reduction in DIN:DIP, as diatoms typically have a high P requirement, e.g., [47,48]. While it may take years for the system to fully adapt to the new nutrient conditions, phytoplankton physiology responds rapidly, whereas the multiple biogeochemical and ecological feedbacks of ecosystem recovery will take multiple seasons to become fully established. Here, initial responses to EchoWater are reported for the fall season, a few months after full implementation, and water quality conditions and phytoplankton physiology are compared to similar times of year for five previous years that varied in flow conditions. Although not all years have availability of precisely the same measured parameters, they do allow us a first look as to how the phytoplankton community responded to changes in nutrients post-upgrade. This first assessment appears to support the hypothesis that alleviation of excessive NH_4^+ loads allowed increased production and less photosynthetic stress.

2. Materials and Methods

2.1. Site Description

The northern San Francisco Estuary, or Bay Delta, consists of the Central Bay, San Pablo Bay, Suisun Bay and the Sacramento-San Joaquin Bay Delta, which is a complex web of rivers, channels, wetlands and floodplains (Figure 1) [49,50]. On a long-term basis, the Sacramento River contributes >80% of the river inflow to the Bay Delta [5]. The sampling herein covered the region of the Sacramento River through Suisun Bay. The Sacramento and San Joaquin Rivers converge at the confluence of the Delta, then flow into Suisun Bay. The mean depths of these regions of the Bay Delta range from 3.3 to 5.7 m [6].

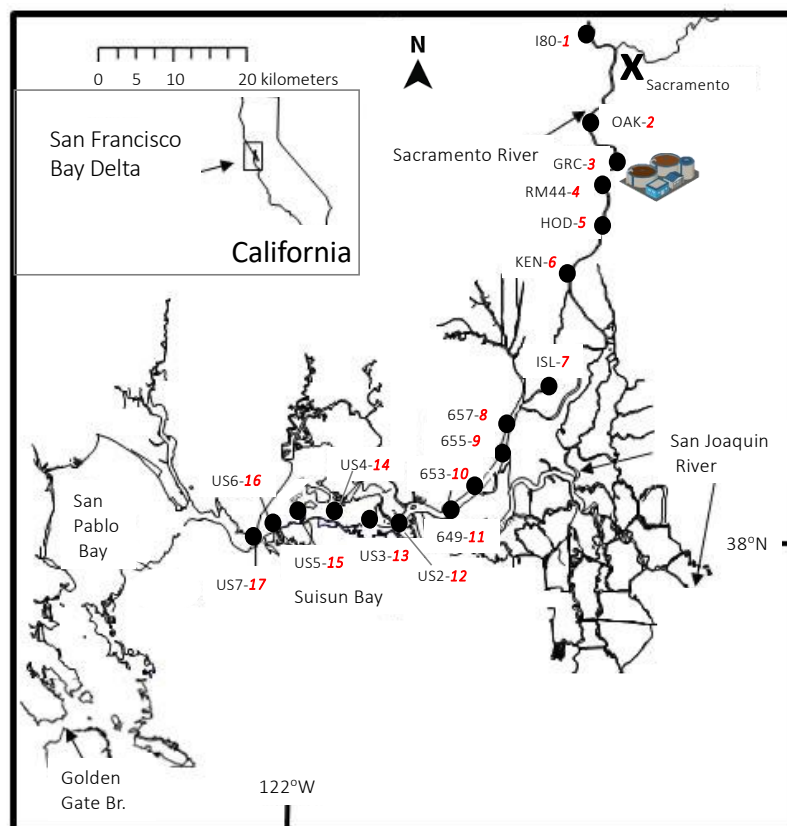


Figure 1. Map of the San Francisco Bay Delta showing the sites sampled over the study years. Each station is identified by a number (in red) and by a regional name. The WWTP that underwent an upgrade and reduction in nitrogen effluent in 2021 is shown with the WWTP icon near Station 3 (GRC). The WWTP icon is from the University of Maryland Integration and Application Network image library.

The dendritic nature of the Sacramento River and the many other tributaries and subestuaries, as well as the specific point source discharges, lead to several natural change points in the river hydrology and ecology [9]. Viewing the river from the upper station, the first change occurs between stations 3 (GRC) and 4 (RM44), where the wastewater is discharged. The next natural change occurs at Station 8 (657), as there is inflow from the Sacramento Ship Channel and other tributaries exit into the Sacramento River between sites 7 (ISL) and Station 8 (657). The next natural change occurs at station 12 (US2), where the Sacramento River exits into Suisun Bay. The San Joaquin River discharges between stations 11 and 12.

2.2. River Flow

Daily river discharge data were downloaded from USGS site 11,455,420 (at Rio Vista (Station 8), www.waterdata.usgs.gov, accessed 15 May 2022). Average values for the 30 days prior to sampling were calculated for each year of sampling.

2.3. Sample Collection

Sampling was undertaken in the months of September or October under the umbrella of three different projects encompassing different years (2011–2013, 2014–2015, 2021). Each sampling period covered stations from above the wastewater treatment plant to Suisun Bay. Although not all stations were sampled on each sampling date, as the different projects had different goals or equipment available, each sampling effort covered the same transect from the upper Sacramento River through Suisun Bay. Stations were identified with varying names, and thus herein, both station number and local name are given for each station reference. Samples were collected on 1-day trips on the R/V Questuary on 6 September 2011, 14 September 2012, 23 September 2013, and on back-to-back 1-day trips encompassing shorter segments of the transects on 15–16 October 2014, 28–30 October 2015 during the pre-upgrade conditions, and five months after full implementation on 22–23 September 2021.

In all years, samples were collected and processed following Wilkerson et al. [25,51]. Samples were collected via a rosette CTD (Seabird Electronics SB-32) equipped with 6, 3-L Niskin bottles. A Secchi disk was used to estimate water clarity. Samples from different depths were collected, but consistently near-surface samples were collected and represent the data herein. All were filtered onboard in duplicate through Whatman GF/F filters (nominally 0.7 μm) for the collection of chl *a* and (except for 2011 and 2021) analysis of phytoplankton diagnostic pigments. Syringe filters (GF/F) were used to collect nutrient samples. Filtrates were stored on ice, and returned to the laboratory for subsequent analysis of NH_4^+ , NO_3^- , PO_4^{3-} and $\text{Si}(\text{OH})_4$.

2.4. Analytical Protocols

Ambient nutrient concentrations were analyzed using manual colorimetric assays (NH_4^+) and autoanalysis techniques ($\text{NO}_3^- + \text{NO}_2^-$ (hereafter NO_3^-), PO_4^{3-} , $\text{Si}(\text{OH})_4$). Concentrations of NH_4^+ were analyzed according to Solorzano [52], while the other nutrients followed Bran and Lubbe protocols [53–55]. Samples for chl *a* were analyzed using a Turner Designs Model 10-AU fluorometer following a 24 h 90% acetone extraction at 4 °C [56]. The fluorometer was calibrated with commercially available chl *a* (Turner Designs).

From 2012 to 2015, phytoplankton pigments were also analyzed using high performance liquid chromatography (HPLC) using methods described by Van Heukelem and Thomas [57]. In 2012 and 2013, samples were processed at the Horn Point Laboratory, University of Maryland Center for Environmental Science (UMCES), and in 2014 and 2015 samples were analyzed at Oregon State University, Corvallis. Although the analysis protocol includes a full suite of pigments, of relevance here are fucoxanthin, chlorophyll *b* (chl *b*), and zeaxanthin, which, when normalized to chl *a*, are a measure of diatoms, green algae, and cyanobacteria, respectively [58,59].

2.5. Photophysiological State and Irradiance Relationships

From 2012 to 2015, a Turner Designs PhytoFlash variable fluorometer was used to assess phytoplankton physiological state. Samples were collected and dark adapted for at least 20 min and measurements of variable fluorescence were taken. Variable fluorescence is the ratio of (F_v) to maximum fluorescence (F_m), F_v/F_m , and is taken as a measure of photosynthetic efficiency, the maximum quantum yield of photosystem II. Reductions in F_v/F_m are taken as a measure of stress in photosystem II. The PhytoFlash provides a single value for the community sample.

In 2021, photophysiological state was measured differently. Samples were collected at each station, kept at ambient temperature under 50–60% irradiance until return to the dock. Samples were then dark acclimated for ~20 min and fluorescence parameters were measured using a Walz PhytoPAM II (Heinz Walz GmbH, Effeltrich, Germany). In contrast to the PhytoFlash instrument, the PhytoPAM II's multiwavelength capability allows deconvolution of signals from different functional groups but does not provide an integrated value for the entire phytoplankton community; it determines the photophysiological condition of each algal group individually. The PhytoPAM II deconvolutes signals associated with brown algae (diatoms and dinoflagellates), green algae, blue-green algae and phycoerythrin-containing algae (e.g., picoplankton such as *Synechococcus*). The instrument was calibrated with diatom, green and phycoerythrin-containing (cyanobacteria) reference spectra. While the brown algal signal includes both diatoms and dinoflagellates, microscopic analyses confirmed that the dominant organism present in this category was diatoms. The major signals that were resolved herein were brown algae (diatoms) and green algae. PE-containing signals were detected at some stations, but values were consistently very low. A non-PE cyanobacterial signal was not resolvable in these samples.

Using the PhytoPAM II, F_v/F_m was first measured for the different algal groups after dark acclimation of ~20 min. Then, the photosynthesis-irradiance response of each sample was measured using the rapid light curve (RLC) function of the PhytoPAM II. RLCs use electron transport rate (ETR) for the currency of photosynthesis and values are expressed as $\mu\text{mol electrons m}^{-2} \text{s}^{-1}$. Samples were exposed to 12 step changes in irradiance at 10 s per step, covering the irradiance range of 5 to 580 $\mu\text{M photons m}^{-2} \text{s}^{-1}$. The ETR of PSII and parameters of the RLCs were calculated using the equation of Platt et al. [60] using the WinControl software package of the PhytoPAM II instrument. For selected stations in 2021, RLCs were conducted with samples that were enriched with variable amounts of NH_4^+ for several hours prior to measurement. The purpose of these experiments was to assess how phytoplankton might have responded in pre-upgrade years if exposed to elevated effluent NH_4^+ .

2.6. Statistical Analyses

Environmental data and photosynthetic parameters were processed in Microsoft Excel or Walz WinControl software. Comparisons were made with ANOVA and Pearson correlations were calculated to examine relationships between parameters.

3. Results

3.1. Flow Conditions

River flow changed substantially over the time period of study. The earlier samplings occurred during non-drought to moderate drought conditions (Figure 2). Over the period of the six studied years, river flow decreased about 3.5-fold when the average discharge of the 30 days prior to sampling was considered. During 2011, when no drought was evident, average flow during the month before sampling was 306 $\text{m}^3 \text{s}^{-1}$, but by 2021, when drought was considered severe, discharge was only 88 $\text{m}^3 \text{s}^{-1}$ (Figure 2).

3.2. Ambient Water Column Conditions

Average water temperatures ranged from a low of 18.5 °C in 2015, the year when sampling was several weeks later than the other years, to 20.8 °C in 2021, when flow was

extremely low. With the exception of 2015, within-transect temperature variability did not generally exceed 2 °C (Figure 3a). Given the several-weeks variability in timing of sampling from year to year, temperature was not related to flow conditions (Figure 3b).

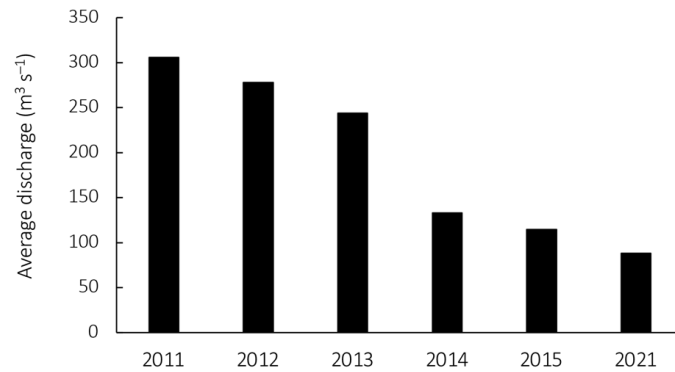


Figure 2. Average discharge at USGS site 11,455,420 at Rio Vista (657, station 8) for the 30-days prior to the date of sampling for each year indicated. Note the clear trend for drier conditions over time.

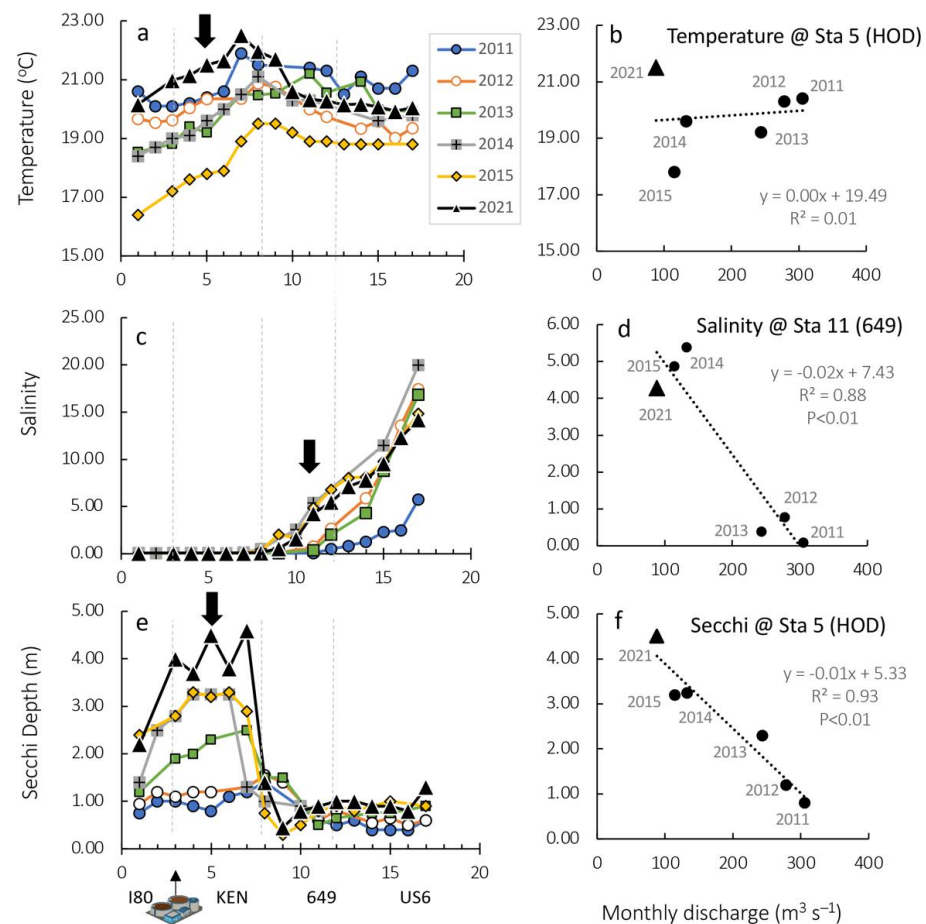


Figure 3. Transects of temperature (panel a), salinity (panel c) and Secchi depth (panel e) for the six years of sampling undertaken in the Bay Delta during September/October. Sampling in 2021 was 5 months after full implementation of the upgraded WWTP. Vertical dashed lines separate the major segments of the river/estuary. The WWTP icon shows location of discharge. Relationships between temperature and flow at Station 5, salinity with flow at Station 11 and Secchi depth with flow at Station 5 are shown in (panels b,d,f), respectively. Note the stations for which relationships with discharge are shown are highlighted by black arrows in (panels a,c,e), and 2021 data in (panels b,d,f) are highlighted by triangles.

Salinity differed significantly between years of sampling (Figure 3c). In 2011, the highest flow year, salinity remained < 6 for the entire transect. In the drier years, salt intrusion was apparent by Station 11 (649), with salinities as high as 5.4 (e.g., 2014). At Station 11, where salt intrusion could be resolved, salinity for all years was significantly related to flow conditions ($R^2 = 0.88$, $p < 0.01$, Figure 3d).

Light availability differed between years and from upriver to down-estuary (Figure 3e). For the first two years of study, 2011 and 2012, the Secchi depth barely exceeded 1 m at any point along the transects. Secchi depth increased with the next two years of study, exceeding 3 m in the upper reach of the river, but dropped to about 1 m in the lower stretch of the transect. Highest Secchi depth was observed in 2021, post upgrade, but this region of relative water clarity was limited to the upper segment of the river. For the four latter years of study, Secchi depth increased from Station 1 (I80) to 3 (GRC), and further increased to Station 7 (ISL) before dropping to values comparable to the other years in the lower section of the transect. At Station 5 (HOD), the Secchi depth for all years of sampling was significantly negatively correlated with monthly discharge ($R^2 = 0.93$, $p < 0.01$, Figure 3f), suggesting that high turbidity was associated with upriver sources (i.e., above Station 1 (I80)), and that with reduced flow, particles were more likely to settle from the water column or were diluted with water from effluent discharge. Station 5 is located a few km south of the WWTP diffusers and represents the first station at which the WWTP effluent is well mixed with the river water.

The nutrients differed significantly between pre- and post-upgrade conditions, and significant differences were also observed with flow conditions. Concentrations of NH_4^+ during the first two years of study, when drought was modest or absent, were $< 30 \mu\text{M}$ near the outfall site (Figure 4a). In 2013, as drier conditions developed, concentrations of NH_4^+ exceeded $50 \mu\text{M}$ near the outfall, and during the drought years prior to upgrade (2014, 2015), concentrations of NH_4^+ near the outfall site were $80\text{--}90 \mu\text{M}$. In the post-upgrade sampling—and consistent with the permit requirements—concentrations of NH_4^+ were $< 5 \mu\text{M}$ throughout the transect. For all years, concentrations of NH_4^+ fell rapidly over the transect and were consistently very low by Station 9 (655) or before. At Station 5 (HOD), concentrations of NH_4^+ for the years prior to upgrade were significantly negatively correlated with flow conditions ($R^2 = 0.98$, $p < 0.01$, Figure 4b), consistent with the notion that the WWTP was the major source of NH_4^+ and concentrations at the point source were diluted with higher flow.

Concentrations of NO_3^- consistently increased down-estuary, but to varying extents from year to year (Figure 4c). Two patterns with distance downstream were apparent. During the higher flow years (2011, 2012, 2013), near-linear increases in NO_3^- concentrations were seen, suggesting a downstream source of this N form or increasing nitrification. For the drier years pre-upgrade (2014, 2015), a sharp transition to elevated NO_3^- concentrations $> 30 \mu\text{M}$ was seen by Station 9 (655), reflecting localized nitrification, with no further increases downriver. Input of NO_3^- from the San Joaquin River is another possible source in this stretch of the estuary. For the EchoWater sample (2021), the peak in concentration at Station 5 (HOD) to $\sim 15 \mu\text{M}$ can be directly attributed to the wastewater discharge. From Station 6 (KEN) through 10 (653), concentrations declined, potentially due to NO_3^- uptake by phytoplankton, then gradually increased through the remainder of the transect stations, reaching concentrations no greater than $\sim 13 \mu\text{M}$. At Station 11 (649), where elevated concentrations of NO_3^- for the years prior to upgrade were apparent, concentrations were significantly negatively correlated with flow conditions ($R^2 = 0.85$, $p < 0.05$, Figure 4d), which would suggest that with reduced flow conditions, more nitrification could be realized.

For PO_4^{3-} during the pre-upgrade years, distinct peaks were recorded at Station 5 (HOD), associated with WWTP discharge (Figure 5a). During the driest year pre-upgrade, 2015, the concentration at this point source was nearly $6 \mu\text{M}$. Concentrations declined over the next few stations (likely due to phytoplankton uptake), then resumed an upward trajectory for the remainder of the river transect, likely reflecting a downstream source.

Although the upgrade did not have a requirement to reduce PO_4^{3-} in the discharge, it appears that such reductions have occurred, with post-upgrade PO_4^{3-} concentrations at the discharge site of $1.3 \mu\text{M}$. At Station 5 (HOD), concentrations of PO_4^{3-} were significantly negatively correlated with flow conditions for the pre-upgrade years ($R^2 = 0.80$, $p < 0.05$, Figure 5b), indicating that the source of PO_4^{3-} was indeed the WWTP.

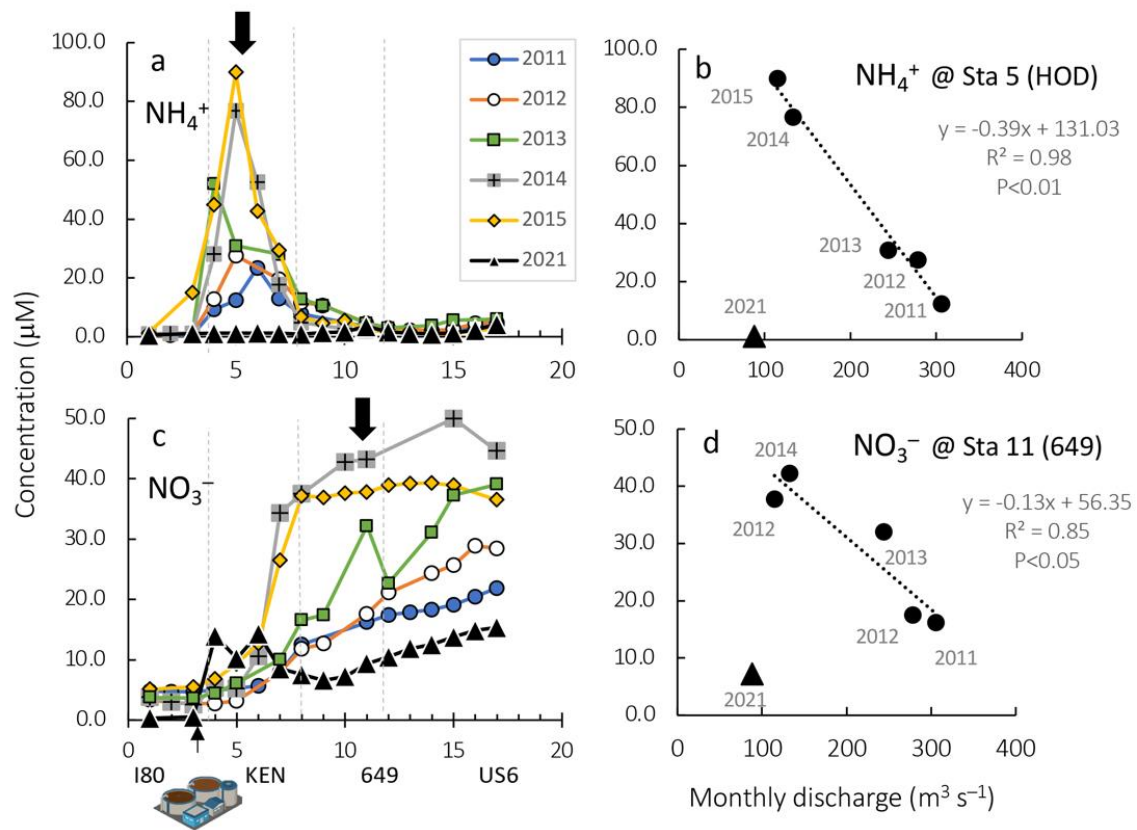


Figure 4. Transects of NH_4^+ (panel a), and NO_3^- (panel c) for the six years of sampling undertaken in the Bay Delta during September/October. Sampling in 2021 was 5 months after full implementation of the upgraded WWTP. Vertical dashed lines separate the major segments of the river/estuary. The WWTP icon shows location of discharge. Correlations of average monthly discharge and NH_4^+ concentrations at station 5 (HOD), and NO_3^- concentrations at station 11 (649), are shown in (panels b,d), respectively. Note the stations for which relationships with discharge are shown are highlighted by black arrows in (panels a,c). The 2021 data (highlighted as triangles) are not included in the regressions.

For all years, all stations, concentrations of $\text{Si}(\text{OH})_4$ remained in the range of $100\text{--}300 \mu\text{M}$, thus at no time was considered limiting or controlling for phytoplankton growth (Figure 5c). During the three latter years when flow was reduced, concentrations of $\text{Si}(\text{OH})_4$ declined more rapidly than during the high flow years, suggestive of increased time for uptake by diatoms (see also below). By Station 11 (649), the concentration of $\text{Si}(\text{OH})_4$ was significantly related to monthly flow over all years ($R^2 = 0.70$, $p < 0.05$, Figure 5d).

3.3. Chlorophyll *a* and Phytoplankton Composition

Concentrations of chl *a* varied considerably between years and sites (Figure 6a). In virtually all years, regardless of flow conditions, concentrations decreased in the first stretch of the river, up to Station 7 (KEN). This would suggest that the river above Station 1 (I80) was a source of chl *a*, and became diluted with wastewater effluent. Thus, at Station 5 (HOD), chl *a* concentrations for all years were significantly and positively related to flow ($R^2 = 0.75$, $p < 0.05$, Figure 6b). Concentrations of chl *a* diverged with distance along the

transect depending on flow and other conditions. For the two higher flow years (2011, 2012), concentrations of chl *a* did not significantly increase in the lower stretch of the transect. In the lowest flow year prior to upgrade (2015), concentrations increased rapidly at Station 8 (657), but then rapidly declined by Station 10 (653). For the post-upgrade sampling, chl *a* increased from Station 7 to 8, and remained high throughout the rest of the river transect, even increasing again in a short-lived peak at Station 16. For 2021, the average chl *a* in the lower river stretch (Stations 2–7) averaged twice ($4.30 \mu\text{g L}^{-1}$) that observed in any of the other years of sampling (mean of $2.14 \mu\text{g L}^{-1}$). Thus, when chl *a* was correlated with flow conditions for Station 11 (649) and Station 14 (US4), no significant relationships were observed (Figure 6c,d). This underscores that algal biomass was not regulated solely by flow.

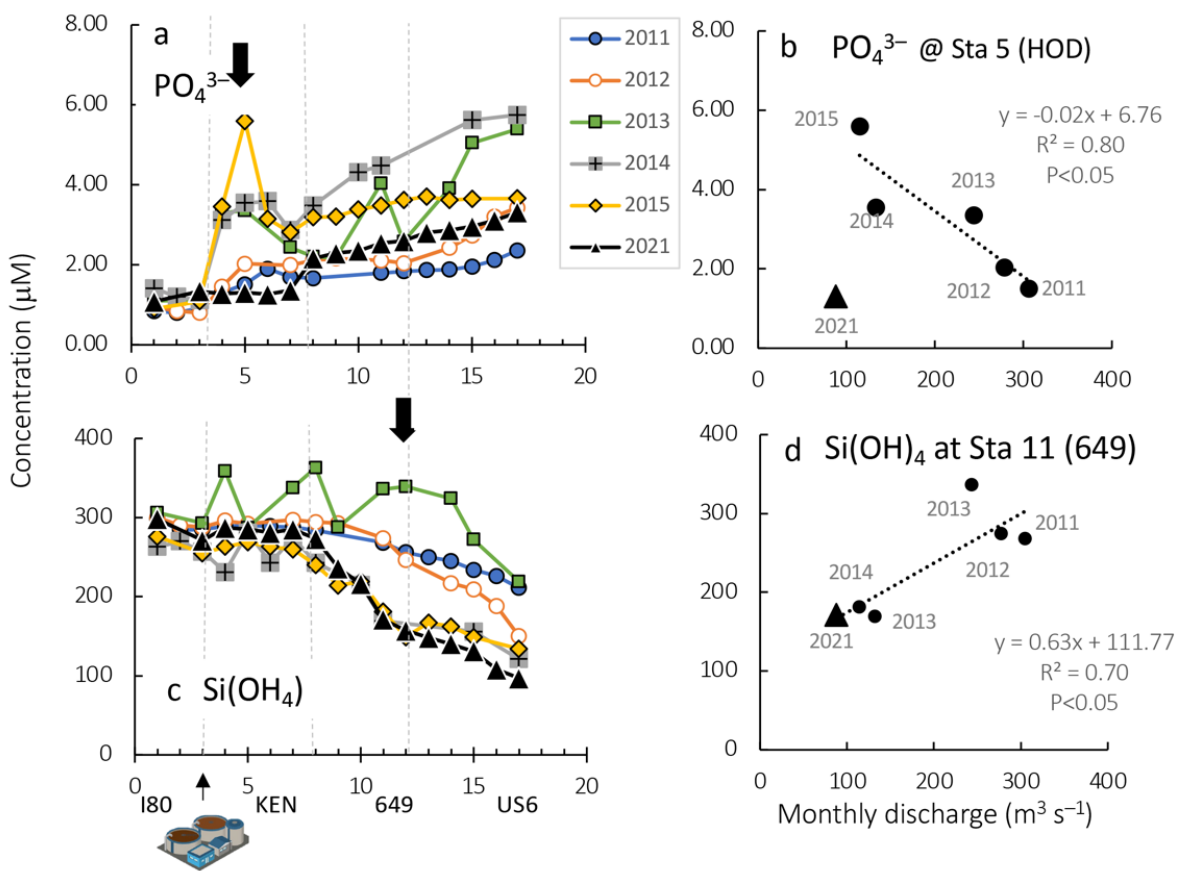


Figure 5. Transects of PO_4^{3-} (panel a) and Si(OH)_4 (panel c) for the six years of sampling undertaken in the Bay Delta during September/October. Sampling in 2021 was 5 months after full implementation of the upgraded WWTP. Vertical dashed lines separate the major segments of the river/estuary. The WWTP icon shows location of discharge. Correlations of average monthly discharge and PO_4^{3-} concentrations at station 5 (HOD), and Si(OH)_4 concentrations at station 11 (649) are shown in (panels b,d), respectively. Note the stations for which relationships with discharge are shown are highlighted by black arrows in (panels a,c). The 2021 data (highlighted as triangles) were not included in the PO_4^{3-} regression.

When chl *a* for all years, all stations, are compared with concentrations of NH_4^+ , a clear decline can be observed with increasing NH_4^+ up to $90 \mu\text{M}$ (Figure 7a). Accumulations of chl *a* above $3 \mu\text{g L}^{-1}$ were witnessed only when ambient concentration of NH_4^+ was $<5 \mu\text{M}$. Indeed, for 2021, when concentrations of NH_4^+ remained $<5 \mu\text{M}$, a significant positive relationship with chl *a* was observed with NH_4^+ availability (Figure 7b). Highest concentrations of chl *a* were also observed when DIN:DIP was in the range of ~ 5 on a molar basis (Figure 7c).

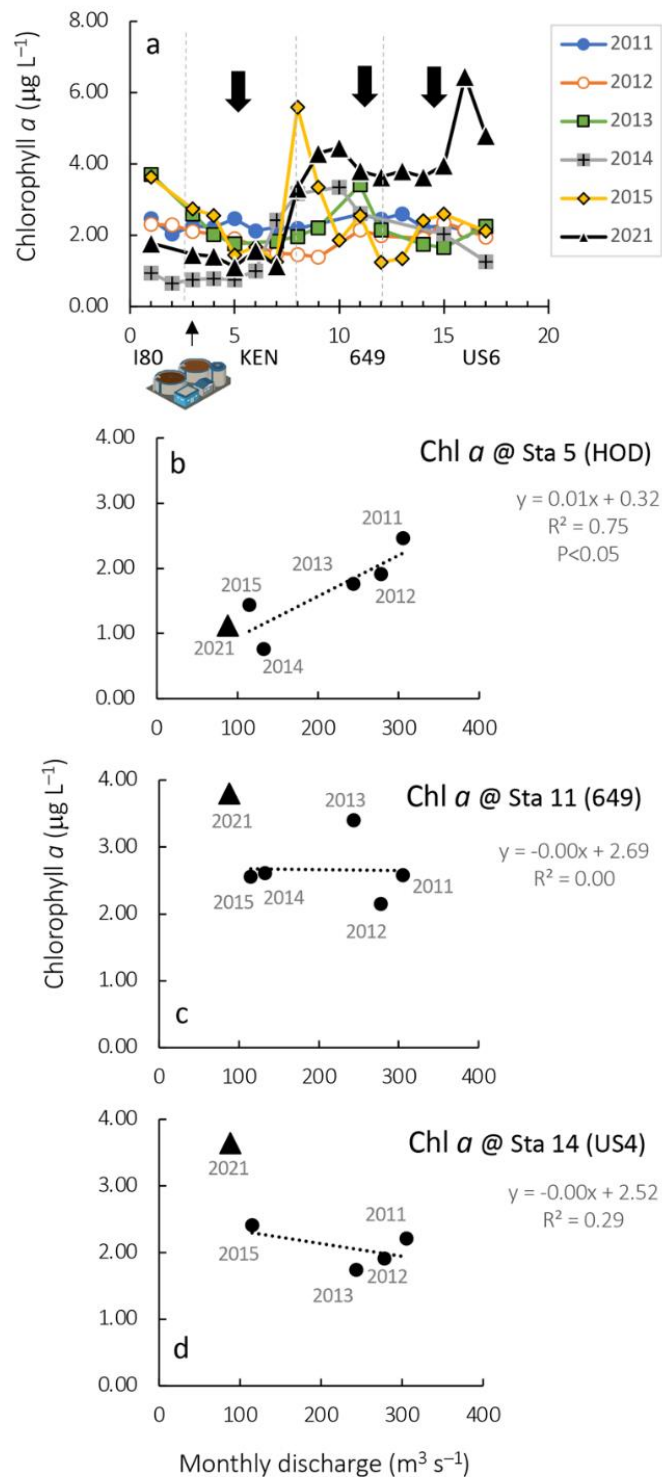


Figure 6. Transects of chlorophyll *a* (panel a) for the six years of sampling undertaken in the Bay Delta during September/October. Sampling in 2021 was 5 months after full implementation of the upgraded WWTP. Vertical dashed lines separate the major segments of the river/estuary. The WWTP icon shows location of discharge. Note the sustained increase in chl *a* after station 7 in 2021, a trend not seen in the other years. The correlations of average monthly discharge and chlorophyll *a* concentrations at station 5 (HOD), at station 11 (649), and at Station 14 (US4) are shown in (panels b–d), respectively. Note the stations for which relationships with discharge are shown are highlighted by black arrows in (panel a).

Table 1. Correlations between chlorophyll *a* and Secchi depth. Relationships for 2012, 2014 and 2021 were significant at $p < 0.05$ (as indicated by bold font).

Year	Correlation	R ²
2011	$Y = -0.18x + 2.44$	0.11
2012	$Y = -0.54x + 2.49$	0.36
2013	$Y = -0.28x + 2.66$	0.08
2014	$Y = -0.88x + 3.45$	0.71
2015	$Y = -0.23x + 2.80$	0.05
2021	$Y = -0.90x + 4.99$	0.77

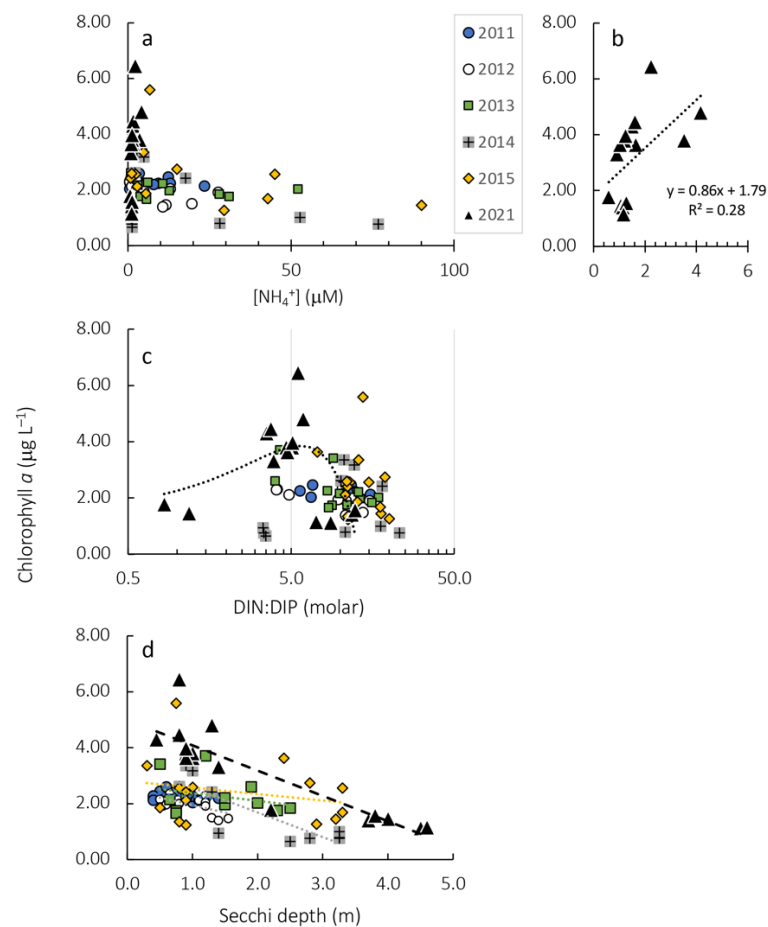


Figure 7. Chlorophyll *a* concentrations for all stations all years as a function of ambient NH_4^+ (panel a; expanded scale for 2021, panel b), as a function of the ambient dissolved inorganic nitrogen:phosphorus ratio (panel c, with the line for 2021 data only), and as a function of secchi depth (panel d). Note the inverse relationships between NH_4^+ concentration (panel a) and light availability (panel d) and chlorophyll *a*. Table 1 summarizes the statistics for (panel d).

When chl *a* for all years, all stations, are compared with light availability (as Secchi depth), an inverse relationship is apparent (Figure 7d, Table 1). This relationship was significant for 2012 ($p < 0.05$), 2014 ($p < 0.01$) and 2021 ($p < 0.001$). Higher light availability in the upper river reaches were related to comparatively lower chl *a* values, and as light decreased with distance along the transect, chl *a* increased. This trend was most apparent for 2021.

Using pigment ratios, the change in phytoplankton composition can be seen to vary between years prior to the WWTP upgrade (Figure 8). For the years prior to WWTP upgrade, the general trend in fucoxanthin/chl *a* was a decline from about Station 5 (HOD) to about Station 10 (653), then an increase for the remainder of the transect (Figure 8a).

For chl *b*/chl *a*, much more variability was observed (Figure 8b). In 2013, there were only moderate fluctuations until Station 12 (US2) when an increase was apparent. In 2014, an increase in the proportion of chl *b*/chl *a* was observed down-estuary from Station 10 (653). In 2015, the driest year prior to WWTP upgrade, a peak was observed at Station 7 (ISL), and a secondary increase was observed at Station 17 (US7).

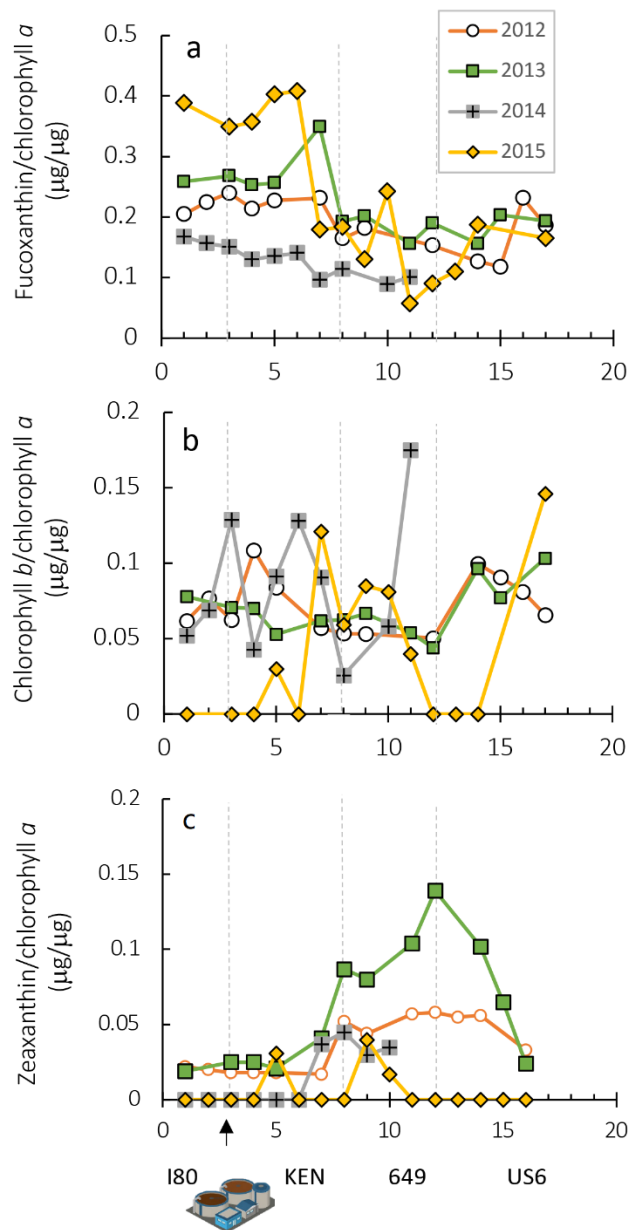


Figure 8. Transects of fucoxanthin/chlorophyll *a* (indicative of diatoms, panel a), chlorophyll *b*/chlorophyll *a* (indication of green algae, panel b) and zeaxanthin/chlorophyll *a* (indicative of cyanobacteria, panel c) for the years of sampling undertaken in the Bay Delta during September/October prior to WWTP upgrade. Vertical dashed lines separate the major segments of the river/estuary. The WWTP icon shows location of discharge.

For the cyanobacterial fraction, reflected in the proportions of zeaxanthin/chl *a*, mid-transect peaks were seen in all years for which data are available (Figure 8c). The peaks were observed to begin in the range of Station 8 (657), and that of 2013 was particularly pronounced. Both 2012 and 2013 were wetter years.

No HPLC data are available for 2021, but an estimate of the relative diatom proportion was made using the rate of depletion of $\text{Si}(\text{OH})_4$ along the lower half of the transects [61]. To do so, the rate of depletion in $\text{Si}(\text{OH})_4$ was calculated for each year using data for the last segment of the estuary, from Stations 11 to 17 (649 to US7) (Table 2). Then, the slopes of those correlations were related to the fucoxanthin/chl *a* data for those years for which HPLC data were available. Using that relationship, the fucoxanthin/chl *a* ratio for 2021 at station 12 was estimated to be 0.16, or 80% higher than the value measured for 2015, the other very dry year.

Table 2. Correlations between $\text{Si}(\text{OH})_4$ and station position, from Stations 11–17. See Figure 5c.

Year	Correlation	R ²
2011	$Y = -8.82x + 364$	0.98
2012	$Y = -16.95x + 453$	0.84
2013	$Y = -9.99x + 426$	0.39
2014	$Y = -10.76x + 308$	0.84
2015	$Y = -10.27x + 301$	0.79
2021	$Y = -16.26x + 367$	0.93

3.4. Photophysiology

For the years prior to upgrade, values of F_v/F_m —although displaying station-to-station variability—generally decreased down-estuary (Figure 9a). A greater decrease, indicative of greater stress, was observed in 2015 relative to 2013. Values for 2014 were much more variable, and actually increased from Stations 10 to 11.

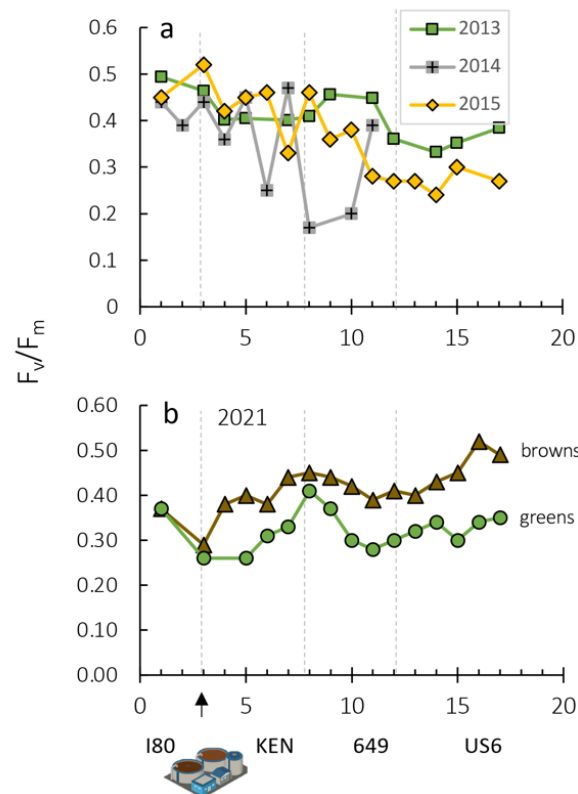


Figure 9. Transects of F_v/F_m for the years of sampling undertaken in the Bay Delta during September/October prior to WWTP upgrade (panel a) and for the brown and green algal groups for 2021 post WWTP upgrade (panel b). Vertical dashed lines separate the major segments of the river/estuary. The WWTP icon shows location of discharge. Note the consistent downward trend for all years pre-upgrade and the upward trend for brown algae for 2021 post-upgrade.

For 2021, the F_v/F_m signal was deconvoluted for the brown (diatom) and green algae (note that the phycoerythrin signal was only discernable in the lower river sites, so a transect for this group of algae is not reported; Figure 9b). F_v/F_m was consistently and significantly higher for the brown compared to the green algae (ANOVA, $p < 0.01$), and neither showed a decline with river position; in fact, there was an increase in the brown F_v/F_m along the transect, from 0.29 at the point source of discharge (Station 3 (GRC) to 0.52 at Station 16 (US6). Comparing the two driest years, 2015 and 2021, at the entrance to Suisun Bay (Station 12, US2), the F_v/F_m for the brown and green algae were 0.41 and 0.30, respectively in 2021, while in 2015, the community F_v/F_m was 0.27.

Rapid light curves conducted in 2021 revealed several patterns and provided several insights into photophysiology. First, for all stations, values of ETR_{max} for the brown algal fraction consistently exceeded those of the green algal fraction (Figure 10, Table 3). Second, for those stations for which experimental manipulations of NH_4^+ were conducted prior to assessment of RLCs, there was a general trend of decreasing ETR_{max} and a decrease in the value of α for the brown algal fraction. For the green algal fraction, changes with enrichment with NH_4^+ were not as consistent, and even increased with NH_4^+ enrichment for some stations. Third, only at the lower estuary sites (Station 17 (US7)) was there a signal that could resolve the phycoerythrin response. An increase in PE-containing cells in this region of the estuary would be consistent with the increase in zeaxanthin/chl *a* observed in 2012 and 2013.

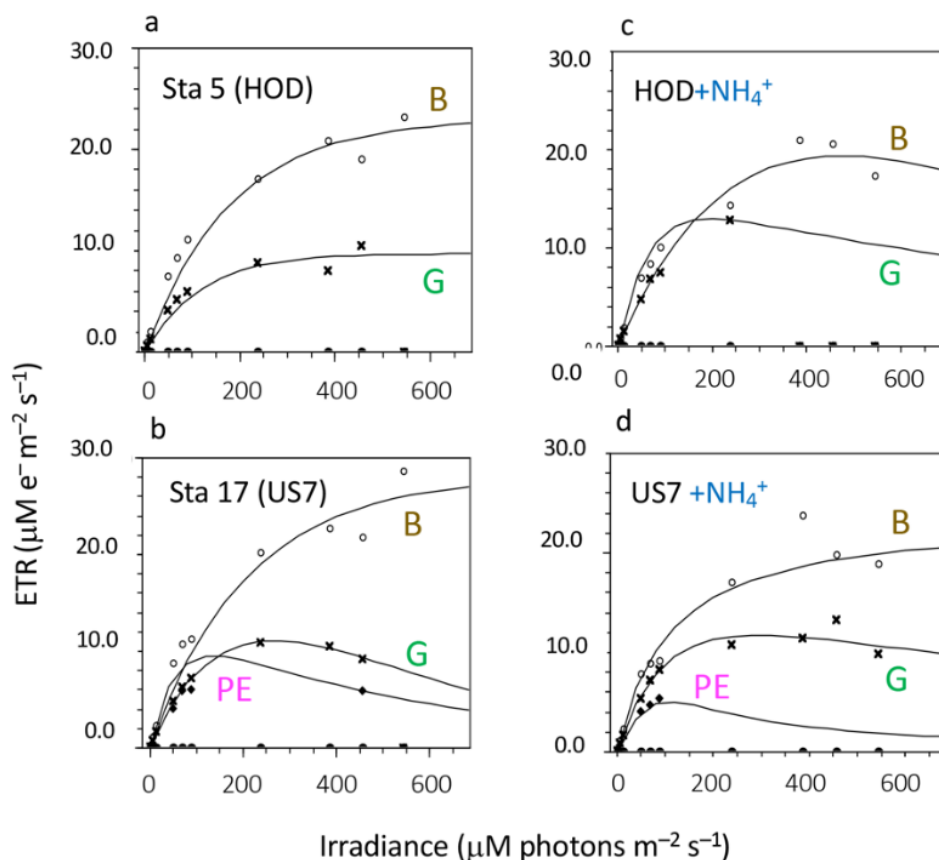


Figure 10. Rapid Light Curves for stations Station 5 (HOD; panel a) and Station 17 (US7; panel b) and the effects of pre-treatment (6 h) with 30 mM NH_4^+ (panels c,d). Curves were generated using Walz WinControl software according to Platt et al. [60]. The algal groups are differentiated as brown (B, diatoms), green (G, chlorophytes) and as phycoerythrin-containing cells (PE). Parameters are summarized in Table 3.

Table 3. Parameters from Rapid Light Curves measured at stations and under conditions indicated. Ambient samples were dark adapted for 20 min. NH_4^+ enriched samples were measured approximately 6 h after enrichment and a 20 min dark acclimation. Algal groups were differentiated by the PhytoPAM II. Ambient concentrations of NH_4^+ are listed for reference.

Station	Treatment	α Brown Algae	ETR_{max} Brown Algae ($\mu\text{M e}^- \text{m}^{-2} \text{s}^{-1}$)	α Green Algae	ETR_{max} Green Algae ($\mu\text{M e}^- \text{m}^{-2} \text{s}^{-1}$)	Ambient NH_4^+ (μM)
1 (I80)	ambient	0.160	26.4	1.761	18.3	0.59
3 (GRC)	ambient	0.158	17.5	0.141	13.4	1.06
4 (RM44)	ambient	0.222	25.0	0.124	18.4	1.14
	+15 $\mu\text{M NH}_4^+$	0.198	23.9	0.175	19.7	
	+30 $\mu\text{M NH}_4^+$	0.197	22.1	0.270	18.1	
	+60 $\mu\text{M NH}_4^+$	0.185	21.5	0.155	17.4	
5 (HOD)	ambient	0.129	23.0	0.084	9.7	1.15
	+30 $\mu\text{M NH}_4^+$	0.111	19.4	0.160	8.0	
6 (KEN)	ambient	0.192	21.4	0.107	13.5	1.27
7 (ISL)	ambient	0.115	15.5	0.138	11.5	1.16
8 (657)	ambient	0.199	29.7	0.177	20.0	0.91
	+30 $\mu\text{M NH}_4^+$	0.184	30.4	0.163	18.4	
9 (655)	ambient	0.183	27.8	0.136	17.2	1.48
10 (653)	ambient	0.175	22.6	0.123	14.3	1.62
11 (649)	ambient	0.142	18.4	0.107	11.2	3.52
12 (US 2)	ambient	0.142	17.7	0.105	13.3	1.65
	+30 $\mu\text{M NH}_4^+$	0.085	13.5	0.148	10.5	
13 (US 3)	ambient	0.114	15.4	0.146	14.4	1.20
14 (US 4)	ambient	0.111	15.6	0.166	13.6	1.03
15 (US 5)	ambient	0.116	14.8	0.175	10.8	1.24
16 (US 6)	ambient	0.145	20.8	0.099	10.9	2.23
17 (US 7)	ambient	0.134	28.1	0.112	11.1	4.17
	+30 $\mu\text{M NH}_4^+$	0.142	20.9	0.090	12.0	

4. Discussion

4.1. Major Trends and Interannual Responses

The role of sewage effluent in the ecology of the Bay Delta has long been a topic of considerable discussion and controversy, e.g., [1,17,18,26–28,38]. The complexity of the Bay Delta system—hydrologically and ecologically—cannot be underestimated. From phytoplankton to fish, the food web of this system has changed significantly over the past several decades [5,6,17,37,62]. Unlike conventional nutrient-impacted systems, the Bay Delta has experienced a decline in productivity as nutrient enrichment has increased over the past several decades. Declines in productivity have been ascribed to multiple causes, ranging from light limitation [37–39], to grazing by invasive clams [6,42,43] and suppressive effects of elevated NH_4^+ on phytoplankton production [1,7,17,18,51]. The Bay Delta ecosystem has also been significantly modified by other invasive species, not only by clams, but also by bay grasses, various species of copepods, and fish over the past several decades [63–65]. The roles of these various stressors need not be mutually exclusive. The WWTP—that had been responsible for the high loads of NH_4^+ to the upper Bay Delta—and its recent upgrade provides an ecosystem test of the hypothesis that NH_4^+ may have negatively impacted productivity over the decades over which it was in operation. The results presented here reflect a “first look” at the system change in the fall season, less than half a year after full implementation of EchoWater. These results reflect short-term phytoplankton responses and do not encompass all the biogeochemical and ecological feedbacks that will become apparent over years. It must be emphasized that the upgrade also occurred during one of the driest years of the past decade and ecosystem responses may also change if and when drought is alleviated.

The major findings emerging from the post-upgrade data are that more chl *a* accumulated in the estuary post-upgrade and, based on photophysiology, phytoplankton appeared

to be less photosynthetically stressed with station position in the lower estuary compared with prior years. Prior to upgrade, concentrations of chl *a* above $\sim 2 \mu\text{g L}^{-1}$ were not observed for any sample collected at any point along the transects in any year if NH_4^+ concentrations were elevated above $5 \mu\text{M}$ regardless of flow conditions, but over that range, chl *a* increased as NH_4^+ increased (Figure 7a,b). In the post-upgrade sampling, when N loadings decreased, concentrations of chl *a* doubled. The more than halving of N loadings also resulted in a comparable reduction in DIN:DIP. Faster phytoplankton growth rates are associated with higher relative proportions of P and more chl *a* was thus associated with a decline in DIN:DIP (Figure 7c), e.g., [48].

Concentrations of chl *a* were also negatively related to Secchi depth, and significantly so for 2012, 2014 and 2021 (Figure 7d). This would suggest, especially for the low flow year of 2021, a down-regulation of chl *a* content as a function of increased light. This finding seemingly contrasts with the notion that low primary production in the Bay Delta is largely controlled by light limitation, e.g., [37–39]. Secchi depths and chl *a* at station 5 (HOD) were significantly negatively correlated with monthly discharge (Figure 3f), further implicating acclimation to ambient conditions as the reason for lower chl *a* values upriver in 2021 compared to other years. From station 10 to 17, the Secchi values for all years were < 1 m, and while modestly higher for 2021, they were not more than a 0.2 m higher than values recorded in 2013, 2014, or 2015. Light availability alone cannot explain the approximately 2-fold higher chl *a* accumulation down-estuary in 2021 compared with all prior studied years.

This study compared data collected in fall when blooms not only have been historically low, but seasonally have been shown to be comparatively rare [66]. The doubling of chl *a* observed here does not represent a bloom, but it was a significant change compared to five prior fall samplings encompassing a range of flow conditions. Fall is also a period when grazing pressure by *Potamocorbula* is likely highest, e.g., [6] but no direct grazing data are available for the post-upgrade period. Observations will be required in additional seasons to fully understand the magnitude of ecosystem effects from nutrient reduction.

The data herein suggest that the elevated NH_4^+ in effluent prior to the WWTP upgrade—reaching concentrations of many tens of μM —impacted phytoplankton in multiple ways. In addition to suppressed chl *a* accumulation, the general trend in F_v/F_m for the samples collected during pre-upgrade years trended downward with distance along the river, indicating stress, while post-upgrade values trended upwards for the brown (diatom) phytoplankton component post-upgrade, indicating increased photosynthetic efficiency (Figure 9). Additionally, the experimental manipulations of samples with NH_4^+ prior to measuring the photosynthetic response indicated a decrease in ETR_{max} and in α in the brown (diatom) fraction of the treated samples compared to the untreated samples (Figure 10, Table 3). The decrease in α values also provides potential insight into light limitation in NH_4^+ -laden waters. Lower α would imply that the cells could not photoacclimate to low light conditions as well. Accordingly, light stress would be more apparent. Diatoms have highly effective non-photochemical quenching (NPQ, xanthophyll cycling) to protect photosynthetic pigments from sudden exposure to high light. Xanthophyll cycling activity in diatoms is much higher than that of higher plants and has been referred to as “super-NPQ” [67]. Previous studies have shown that additions of very high concentrations of NH_4^+ can abolish the formation of NPQ [67]. Future studies will explore NPQ changes in Bay Delta phytoplankton in more detail, and on longer time scales than the RLC experiments conducted here.

Years of different flow, combined with changing nutrient regime, led to differences in the phytoplankton community. In the pre-upgrade years for which pigment data are available, the diatom fraction declined down-estuary, while that of the green algal fraction or the cyanobacterial fraction increased (Figure 8). Many algae and higher plants have lower rates of growth on NH_4^+ than on NO_3^- [34,68] (and references therein). The effect of NH_4^+ on NO_3^- metabolism is complex. It can cause repression of uptake of NO_3^- , it can lead to degradation of nitrate reductase (NR), the enzyme necessary for NO_3^-

assimilation, and it can suppress synthesis of new NR in the cell [29,69,70]. Repression of key NO_3^- enzymes requires time for the cell to recover, and thus along a transect down-estuary—especially when flow is high—cells may not have sufficient time to do so and grow. Cells generally do not de-repress (express an ability to transport and metabolize NO_3^-) unless their internal N status is sufficiently low [71,72]. With exposure to NH_4^+ at the level of 10 s to nearly 100 μM , the internal NH_4^+ concentrations can remain high for an extended time.

Diatoms also have a dependence on the reduction of NO_3^- to NO_2^- in cellular energy balance. They can reduce NO_3^- via NR in a non-assimilatory mode [73–76] and this process serves as a sink for excess reductant that derives from the splitting of water when photochemistry exceeds the assimilatory capacity of the cell. Clearly an important criterion for this pathway to function is the availability of NO_3^- and its key enzymes in the cell. Without this pathway, cells become stressed. This effect likely contributed to the stress seen in the photosynthetic efficiency (F_v/F_m) in the pre-upgrade years. After upgrade, the diatoms were no longer stressed by lack of the NO_3^- reduction pathway to protect the chloroplast from over-reduction. After upgrade, the depletion of $\text{Si}(\text{OH})_4$ increased down-estuary, further suggesting growth by diatoms (Figure 5c).

Green algae and cyanobacteria do not depend on NO_3^- reduction for energy balance in the same way as diatoms. Chlorophytes have well developed Mehler activity for energy balance, and they, as well as cyanobacteria are generally considered to show less stress in the presence of elevated concentrations of NH_4^+ , e.g., [29,77]. Both of these algal groups trended upwards with distance down-estuary (Figure 8b,c).

Building on these physiological pillars, a conceptual model comparing the responses of 2015 and 2021, the driest of the studied years, can be developed (Figure 11). In comparing these years, flow effects can be considered minor. In 2015, the effluent pulse of NH_4^+ was 90 μM (Figure 4a), and in 2021, at the site of effluent discharge it was 1.1 μM . In 2015, although nitrification led to accumulation of NO_3^- of $\sim 40 \mu\text{M}$ through most of the river transect (after Station 7 (ISL)), cellular accumulation of NH_4^+ did not allow diatoms to access this nutrient substrate. Chlorophytes (based on chl *b*/chl *a* ratios) and a short-lived peak of cyanobacteria (based on zeaxanthin/chl *a*) developed in the region of Station 8 (657), but they rapidly declined. Down-estuary in 2015, both diatoms and chlorophytes remained, but in a comparatively more stressed condition, as evidenced by declining photosynthetic efficiency (Figure 9a).

In contrast, in 2021, chl *a* rose after Station 8 (657) and did not decline substantially down-estuary (Figure 6a). Values were approximately twice those observed in previous years. Diatom abundance in Suisun Bay were estimated to be up to 80% higher than in 2015. The diatom photosynthetic efficiency (F_v/F_m) increased. The green algal fraction also showed an increase in F_v/F_m at Station 8 but did not otherwise vary substantially along the transect (Figure 9b).

While the biogeochemical response of the Bay Delta to this ecosystem-scale change in nutrient loads and concentrations will likely play out over longer time scales, the photophysiological response documented here appears to provide a sensitive indicator of changes at the base of the foodweb.

4.2. Importance of Physiological and Ecosystem Scale Experiments

Lessons can be learned from both short-term experimental studies and ecosystem-scale level changes in this and other systems. For example, Berg et al. [26] conducted a laboratory study with species isolated from the Bay Delta, grown on NO_3^- , then exposed to NH_4^+ at varying concentrations in order to mimic the exposures such species would encounter under effluent exposure. However, cultures were not given time to deplete internal pools before physiological measurements were undertaken. Berg et al. [26] did observe variable taxon and concentration effects. Recently, Strong et al. [27] conducted a single 48 h amendment experiment with water from upstream and downstream of the Sacramento wastewater plant prior to upgrade and exposed samples to two light intensities,

50% and 5% of natural irradiance, the latter being light-limiting for growth. They used those data to conclusively state that “ NH_4^+ from wastewater are not likely to be the cause of POD in the Delta... [and that] high anthropogenic NH_4^+ loading from wastewater effluent is not driving the lower productivity and decline of pelagic organisms in the Delta [27] (p. 14). Interestingly, Glibert et al. [24] conducted similar incubation experiments with multiple substrates and light intensities (50% and 15% of natural irradiance) over multiple seasons and years and found that different microbial communities developed when enriched with oxidized vs. chemically reduced forms of N, and that proportionately more chl *a* and fucoxanthin was produced per unit N taken up when enriched with NO_3^- compared to NH_4^+ at reduced light levels. Such a finding may have relevance to the additional chl *a* in the down-estuary sites in 2021 compared with prior years. The comparison of results from these experimental studies [24,26,27] highlights that there is still much to be learned regarding physiological responses and how they can change with experimental treatment and other factors. A key difference in the studies by Strong [27] and Glibert et al. [24] was the use of 5% vs. 15% of surface irradiance as a low light treatment.

The potential for variable responses to NH_4^+ enrichment over time and by different community assemblages was highlighted in a long-term study by Swarbrick et al. [33] in the Qu'Appelle Lakes of the Northern Great Plains of Canada. By using 72 h nutrient bioassays with NH_4^+ , these authors assessed the effects of NH_4^+ over the growing season of two lakes over 16 years (1996–2011), a period during which use of N fertilizer in the watersheds increased. They found that with NH_4^+ enrichment, the phytoplankton responses (as Chl *a*) ranged from a 2691% increase (mean stimulation = $188.1 \pm 365.8\%$) to a 160% suppression (mean suppression = $54.5 \pm 25.7\%$). With time, the frequency of spring suppression and of summer stimulation increased markedly over the studied period. Growth enhancement by NH_4^+ was greatest when phytoplankton communities exhibited a high abundance of chlorophytes, consistent with earlier studies which demonstrate chlorophytes prefer NH_4^+ over other forms of N [24,29,77–79] (and that they can outcompete other taxa for chemically reduced N species when light is sufficient) [80]. In contrast, NH_4^+ pollution was likely to suppress lake production during spring, when low-light adapted phytoplankton (diatoms, cryptophytes, possibly pico-cyanobacteria) predominated.

Other large-scale or mesocosm-level nutrient manipulation experiments further support the notion that dichotomous communities develop in response to comparable NH_4^+ and NO_3^- enrichment. For example, in mesocosm studies Glibert and Berg [81] showed that NO_3^- uptake was directly related to the fraction of the community as diatoms, while the proportion of NH_4^+ uptake was directly proportional to the fraction of the community as cyanobacteria. Domingues et al. [82] also showed that enrichment by NH_4^+ in a freshwater tidal estuary favored chlorophytes and cyanobacteria, whereas diatoms were favored under NO_3^- enrichment. Shangguan et al. [83] showed a shift in phytoplankton taxa to smaller sized cells and a loss of diatoms as NO_3^- availability declined with managed flow changes in lakes near northern Florida Bay. They also showed [84] in mesocosm studies based in Florida Bay that P enrichment along with N in the form of NO_3^- stimulated diatoms while N in the form of NH_4^+ led to picocyanobacteria-dominated communities. Fawcett and Ward [85] showed an acceleration of uptake of NO_3^- by diatoms in mesocosm studies in Monterey Bay, CA, suggesting this to be a mechanism by which diatoms exploit upwelling conditions. In all, various results from short-term nutrient enrichment studies, e.g., [24,84,85], month-long mesocosm experiments [78,86], long-term monitoring [87,88], and mass-balance studies [89,90] from many regions show that effects of N form vary with taxa and environmental conditions at the time of exposure. Cloern [28] has urged caution in interpreting correlations in interpreting causes and effects. We agree and similarly advise caution in disregarding understanding of relationships derived from comparative systems.

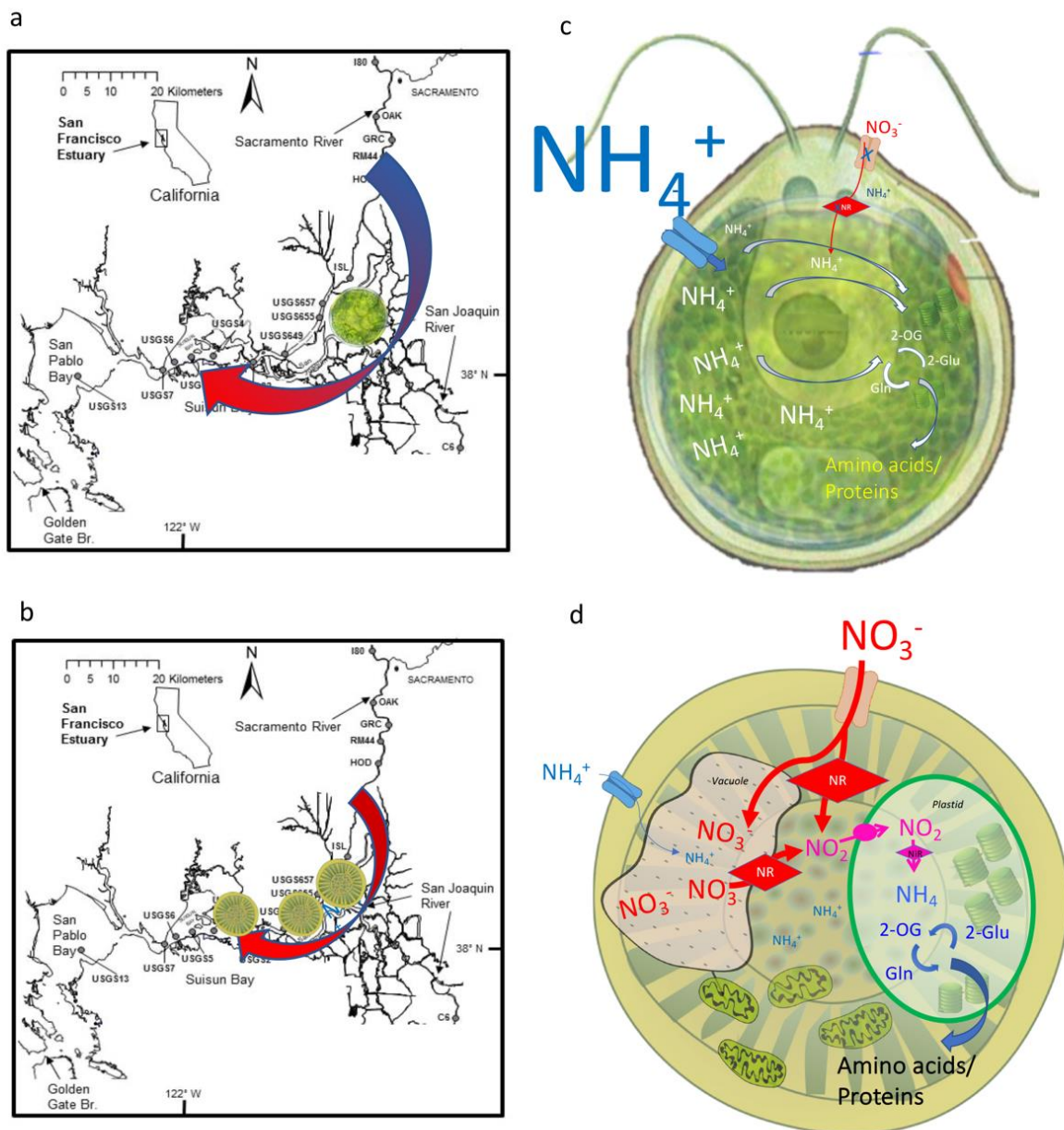


Figure 11. Comparison of the two low-flow years, 2015 (panels a,b) and 2021 (panels c,d), pre- and post-WWTP upgrade. In 2015, there was very high NH_4^+ in the effluent (blue end of arrow in panel a) and nitrification (transition to red in arrow in panel a) occurred by station 8. A peak in chlorophyll *a* developed and was dominated by chlorophytes which were readily able to access the NH_4^+ (panel b) but which could not sustain growth. In 2021, the effluent was in the form of NO_3^- , which remained available through the transect (red arrow in panel c) and was accessible to diatoms (panel d) which were then able to sustain growth through the remainder of the transect. See text for details.

5. Summary

There is no doubt that the Bay Delta will continue to experience multiple stresses in the future and the conversation regarding causes and impacts of various drivers will continue for years to come. The results of this natural ecosystem-scale experiment should be of interest not only to the Bay Delta management community, but to all systems undergoing natural or anthropogenic changes in nutrient loadings, forms and proportions.

In sum, this study has shown that following wastewater improvement and the removal of high NH_4^+ loading from the Sacramento River, there was a significant ecological change

in the river-estuary in contrast to water quality parameters at the same time of year for several years prior to upgrade. It appears that EchoWater had an immediate effect on chl *a* accumulation, and the extent to which this effect continues in the future deserves continual assessment. An increase in chl *a* in the post-upgrade relative to pre-upgrade conditions was associated with cells, especially diatoms, that showed less photosynthetic stress relative to the phytoplankton assemblages in pre-upgrade years. Time will tell whether the Bay Delta estuary recovers to a healthy state, including a healthy food web. These early glimpses into the trajectory of recovery of the important primary producers are promising.

Author Contributions: Conceptualization, P.M.G., F.P.W., R.C.D. and A.E.P.; methodology, P.M.G., F.P.W., R.C.D. and A.E.P.; formal analysis, P.M.G., F.P.W., R.C.D. and A.E.P.; investigation, P.M.G., F.P.W., R.C.D. and A.E.P.; data curation, F.P.W., A.E.P., R.C.D. and P.M.G.; writing—original draft preparation, P.M.G.; writing—review and editing, F.P.W., R.C.D. and A.E.P.; project administration, F.P.W. and P.M.G.; funding acquisition, F.P.W., R.C.D., P.M.G. and A.E.P. All authors have read and agreed to the published version of the manuscript.

Funding: This work was supported by the Delta Stewardship Council (Agreement Number 2038), State and Federal Contractors Water Agency (Agreement Number 12–20), State Water Contractors Agreement Number 20–43, NASA Grant NNX14AD79G and California Department of Fish and Wildlife Agreement Number Q1996035.

Data Availability Statement: Data are being deposited with the Environmental Data Initiative (EDI) <https://environmentaldatainitiative.org/>.

Acknowledgments: We thank S. Blaser, J. Wilson, S. Randall, E. Antell, A. Pimenta, J. Lee, N. Travis, T. Lee, S. Strong (Estuary and Ocean Science Center, San Francisco State University), J. Alexander (UMCES), and S. Murasko (Florida Fish and Wildlife Research Institute) for participation in sample collection on cruises and lab analyses, the Horn Point Analytical Services Laboratory for HPLC data for 2011–2013 and C. O. Davis (Oregon State University) for providing HPLC data for 2014 and 2015, and T. Kana and Bay Instruments, LLC., for providing the PhytoPAM II for use in this project. This is contribution number 6227 from the University of Maryland Center for Environmental Science.

Conflicts of Interest: The funders had no role in the design of the study; in the collection, analyses, or interpretation of data; in the writing of the manuscript; or in the decision to publish the results. PMG is a co-owner of Bay Instruments, LLC.

References

1. Dugdale, R.C.; Wilkerson, F.P.; Hogue, V.E.; Marchi, A. The role of ammonium and nitrate in spring bloom development in San Francisco Bay. *Estuar. Coast. Shelf Sci.* **2007**, *73*, 17–29. [[CrossRef](#)]
2. Sharp, J.H. Marine and aquatic communities, stress from eutrophication. In *Encyclopedia of Biodiversity*; Levine, S., Ed.; Academic Press: Amsterdam, The Netherlands, 2001; Volume 4, pp. 1–11.
3. Yoshiyama, K.; Sharp, J.H. Phytoplankton response to nutrient enrichment in an urbanized estuary: Apparent inhibition of primary production by overeutrophication. *Limnol. Oceanogr.* **2006**, *51*, 424–434. [[CrossRef](#)]
4. Ball, M.D.; Arthur, J.F. Planktonic chlorophyll dynamics in the Northern San Francisco Bay and Delta. In *San Francisco Bay: The Urbanized Estuary*; Conomos, T.J., Ed.; Pacific Division of the American Association for the Advancement of Science: San Francisco, CA, USA, 1979; pp. 265–286.
5. Jassby, A. Phytoplankton in the upper San Francisco Estuary: Recent biomass trends, their causes and their trophic significance. *San Fr. Estuary Watershed Sci.* **2008**, *6*, 1–26. Available online: <https://escholarship.org/uc/item/71h077r1> (accessed on 1 April 2022).
6. Kimmerer, W.J. Open water processes of the San Francisco Estuary: From physical forcing to biological responses. *San Fr. Estuary Watershed Sci.* **2004**, *2*, 1. Available online: <https://escholarship.org/uc/item/9bp499mv> (accessed on 1 April 2022). [[CrossRef](#)]
7. Dugdale, R.; Wilkerson, F.; Parker, A.E.; Marchi, A.; Taberski, K. River flow and ammonium discharge determine spring phytoplankton blooms in an urbanized estuary. *Estuar. Coast. Shelf Sci.* **2012**, *115*, 187–199. [[CrossRef](#)]
8. Dugdale, R.C.; Wilkerson, F.P.; Parker, A.E. A biogeochemical model of phytoplankton productivity in an urban estuary: The importance of ammonium and freshwater flow. *Ecol. Modell.* **2013**, *263*, 291–307. [[CrossRef](#)]
9. Glibert, P.M.; Dugdale, R.C.; Wilkerson, F.; Parjer, A.E.; Alexander, J.; Antell, E.; Blaser, S.; Johnson, A.; Lee, J.; Lee, T.; et al. Major—But rare—Spring blooms in San Francisco Bay Delta, California, a result of the long-term drought, increased residence times, and altered nutrient loads and forms. *J. Exp. Mar. Biol. Ecol.* **2014**, *460*, 8–18. [[CrossRef](#)]
10. Jungbluth, M.; Lee, C.; Patel, C.; Ignoffo, T.; Bergamaschi, B.; Kimmerer, W. Production of the copepod *Pseudodiaptomus forbesi* is not enhanced by ingestion of the diatom *Aulacoseira granulata* during a bloom. *Est. Coasts* **2021**, *44*, 1083–1099. [[CrossRef](#)]

11. Sommer, T.R.; Armor, C.; Baxter, R.; Breuer, R.; Brown, L.; Chotkowski, M.; Culberson, S.; Feyrer, F.; Gingas, M.; Herbold, B.; et al. The collapse of pelagic fishes in the upper San Francisco Estuary. *Fisheries* **2007**, *32*, 270–277. [[CrossRef](#)]
12. Baxter, R.; Breuer, R.; Brown, L.; Conrad, L.; Feyrer, F.; Fong, S.; Gehrts, K.; Grimaldo, L.; Herbold, B.; Hrodey, P.; et al. Interagency Ecological Program 2010 Pelagic Organism Decline Work Plan and Synthesis of Results. Interagency Ecological Program for the San Francisco Estuary. Available online: www.waterboards.ca.gov (accessed on 3 August 2022).
13. Lehman, P.W.; Boyer, G.; Hall, C.; Walker, S.; Gehrts, K. Distribution and toxicity of a new colonial *Microcystis aeruginosa* bloom in the San Francisco Bay Estuary, California. *Hydrobiologia* **2005**, *541*, 87–99. [[CrossRef](#)]
14. Lehman, P.W.; Boyer, G.; Stachwell, M.; Walker, S. The influence of environmental conditions on seasonal variation of *Microcystis* abundance and microcystins concentration in San Francisco Estuary. *Hydrobiologia* **2008**, *600*, 187–204. [[CrossRef](#)]
15. Lehman, P.W.; Kurobe, T.; Lesmeister, S.; Baxa, D.; Tung, A.; Teh, S.J. The impacts of the 2014 severe drought on the *Microcystis* bloom in the San Francisco Estuary. *Harmful Algae* **2017**, *63*, 94–108. [[CrossRef](#)]
16. Van Nieuwenhuysse, E. Response of summer chlorophyll concentration to reduced total phosphorus concentration in the Rhine River (Netherlands) and the Sacramento-San Joaquin Delta (California, USA). *Can. J. Fish. Aqu. Sci.* **2007**, *64*, 1529–1542. [[CrossRef](#)]
17. Glibert, P.M.; Fullerton, D.; Burkholder, J.M.; Cornwell, J.; Kana, T.M. Ecological stoichiometry, biogeochemical cycling, invasive species, and aquatic food webs: San Francisco Estuary and comparative systems. *Rev. Fish. Sci.* **2011**, *19*, 358–417. [[CrossRef](#)]
18. Parker, A.E.; Hogue, V.E.; Wilkerson, F.P.; Dugdale, R.C. Inorganic nitrogen speciation and phytoplankton growth in the high nutrient, low chlorophyll San Francisco Estuary. *Est. Coast. Shelf Sci.* **2012**, *104–105*, 91–101. [[CrossRef](#)]
19. Mosier, A.C.; Francis, C.A. Relative abundance and diversity of ammonia-oxidizing archaea and bacteria in the San Francisco Bay estuary. *Environ. Microb.* **2008**, *10*, 3002–3016. [[CrossRef](#)] [[PubMed](#)]
20. Damashek, J.; Casciotti, K.L.; Francis, C.A. Variable nitrification rates across environmental gradients in turbid, nutrient-rich estuary waters of San Francisco Bay. *Est. Coasts* **2016**, *39*, 1050–1071. [[CrossRef](#)]
21. Sobota, D.J.; Harrison, J.A.; Dahlgren, R.A. Influences of climate, hydrology, and land use on input and export of nitrogen in California watersheds. *Biogeochemistry* **2009**, *94*, 43–62. [[CrossRef](#)]
22. Sobota, D.J.; Harrison, J.A.; Dahlgren, R.A. Linking dissolved and particulate phosphorus export in rivers draining California's Central Valley with anthropogenic sources at the regional scale. *J. Environ. Qual.* **2011**, *40*, 1290–1302. [[CrossRef](#)] [[PubMed](#)]
23. Novick, E.; Senn, D. *External Nutrient Loads to San Francisco Bay*; Contribution No. 704 San Francisco Estuary Institute: Richmond, CA, USA, 2014.
24. Glibert, P.M.; Wilkerson, F.P.; Dugdale, R.C.; Parker, A.E.; Alexander, J.; Blaser, S.; Murasko, S. Microbial communities from San Francisco Bay Delta respond differently to oxidized and reduced nitrogen substrates—Even under conditions that would otherwise suggest nitrogen sufficiency. *Front. Mar. Sci.* **2014**, *1*, 17. [[CrossRef](#)]
25. Wilkerson, F.P.; Dugdale, R.C.; Parker, A.E.; Blaser, S.B.; Pimenta, A. Nutrient uptake and primary productivity in an urban estuary: Using rate measurements to evaluate phytoplankton response to different hydrological and nutrient conditions. *Aquat. Ecol.* **2015**, *49*, 211–233. [[CrossRef](#)]
26. Berg, G.M.; Driscoll, S.; Hayashi, K.; Ross, M.; Kudela, R. Variation in growth rate, carbon assimilation, and photosynthetic efficiency in response to nitrogen source and concentration in phytoplankton isolated from upper San Francisco Bay. *J. Phycol.* **2017**, *53*, 664–679. [[CrossRef](#)]
27. Strong, A.L.; Mills, M.M.; Huang, I.B.; van Dijken, G.L.; Driscoll, S.E.; Berg, G.M.; Kudela, R.M.; Monismith, S.G.; Francis, C.A.; Arrigo, K.R. Response of lower Sacramento River phytoplankton to high-ammonium wastewater effluent. *Elementa* **2021**, *9*, 040. [[CrossRef](#)]
28. Cloern, J.E. Use care when interpreting correlations: The ammonium example in the San Francisco Estuary. *San Fran. Est. Watershed Sci.* **2021**, *19*, 1. [[CrossRef](#)]
29. Glibert, P.M.; Wilkerson, F.P.; Dugdale, R.C.; Raven, J.A.; Dupont, C.L.; Leavitt, P.R.; Parker, A.E.; Burkholder, J.M.; Kana, T.M. Pluses and minuses of ammonium and nitrate uptake and assimilation by phytoplankton and implications for productivity and community composition, with emphasis on nitrogen-enriched conditions. *Limnol. Oceanogr.* **2016**, *61*, 165–197. [[CrossRef](#)]
30. MacIsaac, J.J.; Dugdale, R.C.; Huntsman, S.; Conway, H.L. The effect of sewage on uptake of inorganic nitrogen and carbon by natural populations of marine phytoplankton. *J. Mar. Sci.* **1979**, *37*, 51–66.
31. Waiser, M.J.; Tumber, V.; Holm, J. Effluent-dominated streams. Part 1: Presence and effects of excess nitrogen and phosphorus in Wascana Creek, Saskatchewan, Canada. *Environ. Tox. Chem.* **2011**, *30*, 496–507. [[CrossRef](#)]
32. Xu, J.; Glibert, P.M.; Lui, H.; Yin, K.; Yuan, X.; Chen, M.; Harrison, P.J. Nitrogen sources and rates of phytoplankton uptake in different regions of Hong Kong waters in summer. *Estuaries Coasts* **2012**, *35*, 559–571. [[CrossRef](#)]
33. Swarbrick, V.J.; Simpson, G.L.; Glibert, P.M.; Leavitt, P.R. Differential stimulation and suppression of phytoplankton growth by ammonium enrichment in eutrophic hardwater lakes over 16 years. *Limnol. Oceanogr.* **2019**, *64*, S130–S149. [[CrossRef](#)]
34. Britto, D.T.; Kronzucker, H.J. NH_4^+ toxicity in higher plants: A critical review. *J. Plant Physiol.* **2002**, *159*, 567–584. [[CrossRef](#)]
35. Britto, D.T.; Kronzucker, H.J. Ecological significance and complexity of N-source preference in plants. *Ann. Bot.* **2013**, *112*, 957–963. [[CrossRef](#)] [[PubMed](#)]
36. California Regional Water Quality Control Board Central Valley Region. Waste discharge requirements for the Sacramento Regional County Sanitation District, Permit. R5-2021-0019. Available online: <http://www.waterboards.ca.gov/centralvalley> (accessed on 2 August 2022).

37. Alpine, A.E.; Cloern, J.E. Trophic interactions and direct physical effects control phytoplankton biomass and production in an estuary. *Limnol. Oceanogr.* **1992**, *37*, 946–955. [CrossRef]
38. Cloern, J.E.; Dufford, R. Phytoplankton community ecology: Principles applied in San Francisco Bay. *Mar. Ecol. Prog. Ser.* **2005**, *285*, 1–28. [CrossRef]
39. Cole, B.E.; Cloern, J.E. Significance of biomass and light availability to phytoplankton productivity in San Francisco Bay. *Mar. Ecol. Prog. Ser.* **1984**, *17*, 15–24. [CrossRef]
40. Bever, A.J.; MacWilliams, M.L. Simulating sediment transport processes in San Pablo Bay using coupled hydrodynamic, wave, and sediment transport models. *Mar. Geol.* **2013**, *345*, 235–253. [CrossRef]
41. Schoellhamer, D.H.; Wright, S.A.; Drexler, J. A conceptual model of sedimentation in the Sacramento–San Joaquin Delta. *San Franc. Estuary Watershed Sci.* **2012**, *10*. Available online: <https://escholarship.org/uc/item/2652z8sq> (accessed on 12 May 2022). [CrossRef]
42. Kimmerer, W.J.; Thompson, J.K. Phytoplankton growth balanced by clam and zooplankton grazing and net transport into the low-salinity zone of the San Francisco Estuary. *Est. Coasts* **2014**, *37*, 1202–1218. [CrossRef]
43. Lucas, L.V.; Cloern, J.E.; Thompson, J.K.; Stacey, M.T.; Koseff, J.R. Bivalve grazing can shape phytoplankton communities. *Front. Mar. Sci.* **2016**, *3*, 14. [CrossRef]
44. Huber, M. *Potamocorbula amurensis* (Schrenck, 1981). In *World Marine Mollusca Database*; Bouchet, P., Gofas, S., Rosenberg, G., Eds.; 2010. Available online: <http://www.marinespecies.org/aphia.php?p=taxdetails&id=397175> (accessed on 13 May 2022).
45. Lucas, L.V.; Thompson, J.K.; Brown, L.R. Why are diverse relationships observed between phytoplankton biomass and transport time? *Limnol. Oceanogr.* **2009**, *54*, 381–390. [CrossRef]
46. Wang, Z.; Chai, F.; Dugdale, R.; Liu, Q.; Xue, H.; Wilkerson, F.; Chao, Y.; Zhang, Y.; Zhang, H. The interannual variabilities of chlorophyll and nutrients in San Francisco Bay: A modeling study. *Ocean Dyn.* **2020**, *70*, 1169–1186. [CrossRef]
47. Klausmeier, C.A.; Litchman, E.; Daufresne, T.; Levin, S.A. Phytoplankton stoichiometry. *Ecol. Res.* **2008**, *23*, 479–485. [CrossRef]
48. Hillebrand, H.; Steinert, G.; Boersma, M.; Malzahn, A.; Meunier, C.L.; Plum, C.; Ptacnik, R. Goldman revisited: Faster-growing phytoplankton has lower N:P and lower stoichiometric flexibility. *Limnol. Oceanogr.* **2013**, *58*, 2076–2088. [CrossRef]
49. Atwater, B.F.; Conard, S.G.; Dowden, J.N.; Hedel, C.W.; MacDonald, R.L.; Savage, W. History, landforms, and vegetation of the estuary’s tidal marshes. In *San Francisco Bay: The Urbanized Estuary*; Conomos, T.J., Ed.; Pacific Division of the American Association for the Advancement of Science: San Francisco, CA, USA, 1979; pp. 347–385.
50. Mueller-Solger, A.B.; Jassby, A.D.; Müller-Navarra, D. Nutritional value of particulate organic matter for zooplankton (*Daphnia*) in a tidal freshwater system (Sacramento-San Joaquin River Delta, USA). *Limnol. Oceanogr.* **2002**, *47*, 1468–1476. [CrossRef]
51. Wilkerson, F.P.; Dugdale, R.C.; Hogue, V.E.; Marchi, A. Phytoplankton blooms and nitrogen productivity in San Francisco Bay. *Est. Coasts* **2006**, *29*, 401–416. [CrossRef]
52. Solórzano, L. Determination of ammonia in natural waters by the phenolhypochlorite method. *Limnol. Oceanogr.* **1969**, *14*, 799–801. [CrossRef]
53. Bran Luebbe, Inc. *Bran Luebbe AutoAnalyzer Applications: AutoAnalyzer Method No. G-172-96 Nitrate and Nitrite in Water and Seawater*; Bran Luebbe, Inc.: Buffalo Grove, IL, USA, 1999.
54. Bran Luebbe, Inc. *Bran Luebbe AutoAnalyzer Applications: AutoAnalyzer Method No. G-175-96 Phosphate in Water and Seawater*; Bran Luebbe, Inc.: Buffalo Grove, IL, USA, 1999.
55. Bran Luebbe, Inc. *Bran Luebbe AutoAnalyzer Applications: AutoAnalyzer Method No. G-177-96 Silicate in Water and Seawater*; Bran Luebbe, Inc.: Buffalo Grove, IL, USA, 1999.
56. Arar, E.J.; Collins, G.B. In Vivo Determination of Chlorophyll a and Phaeophytin a in Marine and Freshwater Phytoplankton by Fluorescence, Method 445.0. U.S. In *In Vivo Determination of Chlorophyll a and Phaeophytin a in Marine and Freshwater Phytoplankton by Fluorescence, Method 445.0. U.S.*; Environmental Protection Agency: Washington, DC, USA, 1997. Available online: https://cfpub.epa.gov/si/si_public_record_report.cfm?Lab=NERL&dirEntryId=309417 (accessed on 22 September 2021).
57. Van Heukelem, L.; Thomas, C.S. Computer-assisted high-performance liquid chromatography method development with applications to the isolation and analysis of phytoplankton pigments. *J. Chromatogr.* **2001**, *910*, 31–49. [CrossRef]
58. Jeffrey, S.W.; Wright, S.W. Photosynthetic pigments in the haptophyta. In *The Haptophyte Algae*; Green, J.C., Leadbeater, B.S.C., Eds.; Clarendon Press: Oxford, UK, 1994; pp. 111–132.
59. Jeffrey, S.W.; Vesik, M. Introduction to marine phytoplankton and their pigment signatures. In *Phytoplankton Pigments in Oceanography: Guidelines to Modern Methods*; Jeffrey, S.W., Mantoura, R.F.C., Wright, S.W., Eds.; UNESCO: Paris, France, 1997; pp. 37–84.
60. Platt, T.; Gallegos, C.; Harrison, W.G. Photoinhibition of photosynthesis in natural assemblages of marine phytoplankton. *J. Mar. Res.* **1980**, *38*, 687–701.
61. Kimmerer, W. Long-term changes in apparent uptake of silica in the San Francisco estuary. *Limnol. Oceanogr.* **2005**, *50*, 793–798. [CrossRef]
62. Jassby, A.D.; Cloern, J.E.; Cole, B.E. Annual primary production: Patterns and mechanisms of change in a nutrient-rich tidal ecosystem. *Limnol. Oceanogr.* **2002**, *47*, 698–712. [CrossRef]
63. Carlton, J.T.; Thompson, J.K.; Schemel, L.E.; Nichols, F.H. Remarkable invasion of San Francisco Bay (California, USA) by the Asian clam, *Potamocorbula amurensis*. 1. Invasion and dispersal. *Mar. Ecol. Prog. Ser.* **1990**, *66*, 81–94. [CrossRef]

64. Cohen, A.N.; Carlton, J.T. *Nonindigenous Aquatic Species in a United States Estuary: A case study of the Biological Invasions of the San Francisco Bay and Delta*; U.S. Fish & Wildlife Service: Washington, DC, USA, 1995.
65. Cohen, A.N.; Carlton, J.T. Accelerating invasion rate in a highly invaded estuary. *Science* **1998**, *279*, 555–558. [[CrossRef](#)]
66. Brown, L.R.; Baxter, R.; Castillo, G.; Conrad, L.; Culberson, S.; Erickson, G.; Feyrer, F.; Fong, S.; Gehrts, K.; Grimaldo, L.; et al. *Synthesis of Studies in the Fall Low-Salinity Zone of the San Francisco Estuary, September–December 2011: U.S. Geological Survey Scientific Investigations Report 2014–5041*; U.S. Geological Survey: Reston, VA, USA, 2014.
67. Ruben, A.V.; Lavaud, J.; Rousseau, B.; Guglielmi, G.; Horton, P.; Etienne, A.L. The super-excess energy dissipation in diatom algae: Comparative analysis with higher plants. *Photosyn. Res.* **2004**, *82*, 165–175. [[CrossRef](#)] [[PubMed](#)]
68. Raven, J.A.; Wollenweber, B.; Handley, L.L. A comparison of ammonium and nitrate as nitrogen sources for photolithotrophs. *New Phytol.* **1992**, *121*, 19–32. [[CrossRef](#)]
69. Flynn, K.J.; Fasham, M.J.R.; Hipkin, C.R. Modelling the interactions between ammonium and nitrate uptake in marine phytoplankton. *Phil. Trans. R Soc. Ser. B* **1997**, *352*, 1625–1645. [[CrossRef](#)]
70. Vergera, J.; Berges, J.; Falkowski, P. Diel periodicity of nitrate reductase activity and protein levels in the marine diatom *Thalassiosira weissflogii* (Bacillariophyceae). *J. Phycol.* **1998**, *34*, 952–961. [[CrossRef](#)]
71. Flynn, K.J.; Dickson, D.M.J.; Al-Amoundi, O.A. The ratio of glutamine:glutamate in microalgae: A biomarker for N-status suitable for use at natural densities. *J. Plankt. Res.* **1989**, *11*, 165–170. [[CrossRef](#)]
72. Flynn, K.J.; Jones, K.J.; Raine, R.; Richard, J.; Flynn, K. Use of intracellular amino acids as an indicator of the physiological status of natural dinoflagellate populations. *Mar. Ecol. Prog. Ser.* **1994**, *103*, 175–186. [[CrossRef](#)]
73. Lomas, M.W.; Glibert, P.M. Temperature regulation of nitrate uptake: A novel hypothesis about nitrate uptake and reduction in cool-water diatoms. *Limnol. Oceanogr.* **1999**, *44*, 556–572. [[CrossRef](#)]
74. Lomas, M.W.; Glibert, P.M. Interactions between NH_4^+ and NO_3^- uptake and assimilation: Comparison of diatoms and dinoflagellates at several growth temperatures. *Mar. Biol.* **1999**, *133*, 541–551. [[CrossRef](#)]
75. Parker, M.S.; Armbrust, E.V. Synergistic effects of light, temperature and nitrogen source on transcription of genes for carbon and nitrogen metabolism in the centric diatom *Thalassiosira pseudonana* (Bacillariophyceae). *J. Phycol.* **2005**, *41*, 1142–1153. [[CrossRef](#)]
76. Kamp, A.; de Beer, D.; Nitsch, J.L.; Lavik, G.; Stief, P. Diatoms respire nitrate to survive dark and anoxic conditions. *Proc. Natl. Acad. Sci. USA* **2011**, *108*, 5649–5654. [[CrossRef](#)] [[PubMed](#)]
77. Collos, Y.; Harrison, P.J. Acclimation and toxicity of high ammonium concentrations to unicellular algae. *Mar. Poll. Bull.* **2014**, *80*, 8–23. [[CrossRef](#)] [[PubMed](#)]
78. Finlay, K.; Patoine, A.; Donald, D.B.; Bogard, M.; Leavitt, P.R. Experimental evidence that pollution with urea can degrade water quality in phosphorus-rich lakes of the Northern Great Plains. *Limnol. Oceanogr.* **2010**, *55*, 1213–1230. [[CrossRef](#)]
79. Donald, D.B.; Bogard, M.J.; Finlay, K.; Bunting, L.; Leavitt, P.R. Phytoplankton-specific response to enrichment of phosphorus-rich surface waters with ammonium, nitrate, and urea. *PLoS ONE* **2013**, *8*, e53277. [[CrossRef](#)]
80. Jensen, J.P.; Jeppesen, E.; Orlík, K.; Kristensen, P. Impact of nutrients and physical factors on the shift from cyanobacteria to chlorophyte dominance in shallow Danish lakes. *Can. J. Fish. Aquat. Sci.* **1994**, *51*, 1692–1699. [[CrossRef](#)]
81. Glibert, P.M.; Berg, G.M.B. Nitrogen form, fate and phytoplankton composition. In *Experimental Ecosystems and Scale: Tools for Understanding and Managing Coastal Ecosystems*; Kennedy, V.S., Kemp, W.M., Peterson, J.E., Dennison, W.C., Eds.; Springer: New York, NY, USA, 2009; pp. 183–189.
82. Domingues, R.B.; Barbosa, A.B.; Sommer, U.; Galvão, H.M. Ammonium, nitrate and phytoplankton interactions in a freshwater tidal estuarine zone: Potential effects of cultural eutrophication. *Aquat. Sci.* **2011**, *73*, 331–343. [[CrossRef](#)]
83. Shangquan, Y.; Glibert, P.M.; Alexander, J.A.; Madden, C.J.; Murasko, S. Nutrients and phytoplankton in semi-enclosed lagoon systems in Florida Bay and their responses to changes in flow from Everglades restoration. *Limnol. Oceanogr.* **2017**, *62*, S327–S347. [[CrossRef](#)]
84. Shangquan, Y.; Glibert, P.M.; Alexander, J.A.; Madden, C.J.; Murasko, S. Phytoplankton community response to changing nutrients in Florida Bay: Results of mesocosm studies. *J. Exp. Mar. Biol. Ecol.* **2017**, *494*, 38–53. [[CrossRef](#)]
85. Fawcett, S.E.; Ward, B.B. Phytoplankton succession and nitrogen utilization during the development of an upwelling bloom. *Mar. Ecol. Prog. Ser.* **2011**, *428*, 13–31. [[CrossRef](#)]
86. Donald, D.B.; Bogard, M.J.; Finlay, K.; Leavitt, P.R. Comparative effects of urea, ammonium, and nitrate on phytoplankton abundance, community composition, and toxicity in hypereutrophic freshwaters. *Limnol. Oceanogr.* **2011**, *56*, 2161–2175. [[CrossRef](#)]
87. Dai, G.-Z.; Shang, J.-L.; Qiu, B.-S. Ammonia may play an important role in the succession of cyanobacterial blooms and the distribution of common algal species in shallow freshwater lakes. *Glob. Change Biol.* **2012**, *18*, 1571–1581. [[CrossRef](#)]
88. Vogt, R.J.; Rusak, J.A.; Patoine, A.; Leavitt, P.R. Differential effects of energy and mass influx on the landscape synchrony of lake ecosystems. *Ecology* **2011**, *92*, 1104–1114. [[CrossRef](#)] [[PubMed](#)]
89. Leavitt, P.R.; Brock, C.S.; Ebel, C.; Patoine, A. Landscape-scale effects of urban nitrogen on a chain of freshwater lakes in central North America. *Limnol. Oceanogr.* **2006**, *51*, 2262–2277. [[CrossRef](#)]
90. Patoine, A.; Graham, M.D.; Leavitt, P.R. Spatial variation of nitrogen fixation in lakes of the northern Great Plains. *Limnol. Oceanogr.* **2006**, *51*, 1665–1677. [[CrossRef](#)]